PNE-951

CABRIOLET

CLOSE-IN AIR BLAST FROM THE CABRIOLET EVENT

Issuance Date: October 25, 1968

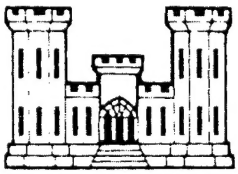

U.S. ARMY CORPS OF ENGINEERS
SANDIA CORPORATION
ALBUQUERQUE, NEW MEXICO

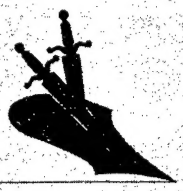

PLOWSHARE

UNITED STATES ATOMIC ENERGY COMMISSION

CIVIL, INDUSTRIAL AND SCIENTIFIC USES FOR NUCLEAR EXPLOSIVES

LEGAL NOTICE

Printed in USA. Price $3.00. Available from the Clearinghouse for Federal Scientific and Technical Information, National Bureau of Standards, U. S. Department of Commerce, Springfield, Virginia 22151.

USAEC Division of Technical Information Extension, Oak Ridge, Tennessee

PNE-951
NUCLEAR EXPLOSIONS - PEACEFUL APPLICATIONS (TID-4500)

PROJECT CABRIOLET

CLOSE-IN AIR BLAST FROM THE CABRIOLET EVENT

L. J. Vortman
Sandia Corporation
Albuquerque, New Mexico

July 1968

ABSTRACT

Results are given of pressure-time measurements measured by two gages at each of eight stations from surface ground zero to 6000 feet on the Cabriolet event. The largest overpressures resulted from the air-transmitted ground-shock-induced pulse and were comparable to those measured on the Danny Boy and Sulky events. There is evidence that for underground explosions as for aboveground explosions the air blast from a 1-kiloton nuclear explosion is comparable to that from 1/2 kiloton of TNT. The weak pulse from venting gas was also comparable to those from Danny Boy and Sulky and all were well below those from comparable TNT explosions. Comparisons between airblast from Cabriolet and that from Palanquin in the same medium are made.

FOREWORD

"This document is the author's report to the Technical Director of Project Cabriolet. The findings and conclusions contained herein are those of the author and are not necessarily those of the Atomic Energy Commission. Accordingly, references to this material must cite the author."

ACKNOWLEDGMENTS

These measurements of the Cabriolet air blast were obtained by B. C. Holt. He was assisted in the planning and engineering by H. G. Larsen. The data were reduced by J. L. Martinez. J. M. Levesque prepared the playbacks presented herein.

TABLE OF CONTENTS

CLOSE-IN AIR BLAST FROM THE CABRIOLET EVENT

CHAPTER 1 - INTRODUCTION

1.1 Description of the Cabriolet Event

Project Cabriolet was a nuclear experiment in hard, dry rhyolite rock executed as a part of the Plowshare Program for development of nuclear excavation. Cabriolet was detonated on January 26, 1968, at approximately 0800:00.105 (PST), 1600:00.105 (GMT), in Area 20, Nevada Test Site (NTS). The resultant yield was 2.3 ± 0.5 kilotons. The emplacement hole was U201 at geodetic coordinates:

Longitude: W 116° 30' 52.0082"
Latitude: N 37° 16' 51.0715"

Surface ground zero (GZ) was 6197 feet MSL; emplacement depth (to the working point) was 170.75 feet. The resultant crater was characterized by the following dimensions and volumes:

1.	Radius of apparent crater (R_a)	54.68 meters 179.4 ft
2.	Maximum depth of apparent crater (D_a)	35.48 meters 116.4 ft
3.	Average apparent crater lip crest height (H_{al})	9.69 meters 31.8 ft
4.	Radius of apparent lip crest (R_{al})	65.14 meters 213.7 ft
5.	Radius of outer boundary of continuous ejecta (R_{eb})	201 meters 660 ft
6.	Lip volume, apparent	184,900 cubic meters 241,887 cubic yards
7.	Crater volume, apparent (V_a)	137,600 cubic meters 180,025 cubic yards

1.2 Objectives

The objectives of the close-in air blast experiment were:

a. To measure close-in air blast as a function of distance from a nuclear explosion in hard rock, the measurements of which could be compared with those from the Palanquin event,

b. To compare these measurements with results from earlier HE and NE detonations in hard rock and other media, and

c. To establish blast suppression as a function of charge burial as one constituent of a model for predicting blast from large-yield nuclear explosions.

1.3 Background

Close-in air blast from single TNT shots in hard rock (Project Buckboard[1]) showed little difference from that of single TNT shots in alluvial soil (Project Stagecoach[2] and Project Scooter[3]). Both exhibited two waves propagated at sonic velocity in air, one due to the piston action of the ground shock at the epicenter followed by a second larger pulse due to venting gases. Project Danny Boy[4,5], the first nuclear cratering experiment in hard rock (0.43 kiloton at 115 feet), gave signals in which, by contrast, the initial wave was the larger. Lack of an accurate time base on the records prevented positive identification of larger constituents of the wave. Projects Dugout[6] (a row of five 20-ton nitromethane charges buried 59 feet and spaced 45 feet apart), Sulky[7] (a single 0.085-kiloton nuclear charge at 90 feet), and Palanquin[8] (a single 4.3-kiloton nuclear charge at 280 feet), records were accurately timed and provided the opportunity for positive identification of four constituents of the blast wave, which were as follows:

a. A ground-transmitted, ground-shock-induced pulse, which is maximum at the epicenter, propagated radially from the explosion at sonic velocity in rock. Because the ground shock attenuates rapidly with distance, so also does the air blast it generates. The attenuation rate of the induced air pulse is further increased because only the vertical component of ground motion will generate air blast, and that component decreases rapidly with decreases in the ratio of burial depth to distance. The direct ground-shock-induced pulse was not positively identified from arrival times on either the Dugout or Sulky shots because of the great spacing between the epicenter and the closest gage. However, it may have been indicated by a larger-than-expected peak overpressure at the closest gage station on each event. The pulse was recognized at the ground zero station on the Palanquin event.

b. A Rayleigh-wave-induced pulse was observed from the closest to the most distant stations on the Dugout, Sulky, and Palanquin events. This pulse propagated in basalt at about 4500 ft/sec--slower than the shock velocity in rock but faster than that in the air. On the Palanquin event, the velocity in rhyolite was about 4900 ft/sec.

c. The air-transmitted, ground-shock-induced pulse is, at the epicenter, the same as the ground-transmitted, ground-shock-induced pulse. From the epicenter, however, it propagates outward at shock velocity in air rather than at the velocity through the ground. For Projects Palanquin, Sulky, and Dugout, it was the dominant wave, and it is presumed to have been the dominant pulse for Danny Boy.

d. The final pulse is that due to venting gases. On Palanquin, Sulky, and Dugout, the arrival coincided with the negative phase following the preceding air-transmitted, ground-shock-induced pulse. A double pulse was observed on the Palanquin event. Because of this and the small amount of gas created by the nuclear explosion, the peak overpressures from the Sulky gas venting pulse did not rise above ambient pressure.

In addition to the principal objectives, Cabriolet, like Palanquin, was designed to shed light on air blast at the epicenter and in the region between the epicenter and the closest previous measurement, especially to identify both the ground-transmitted, ground-shock-induced pulse and the development of the Rayleigh-wave-induced-pulse.

In the formation of the crater from the 280-foot deep Palanquin shot erosion from venting gases[9] appears to have played a larger part than on previous cratering events. For this reason the air blast from venting gases of Palanquin may not be precisely comparable to that of the earlier shots. Thus, one of the gains to be made from the Cabriolet event is an evaluation of the uniqueness of the air blast from Palanquin.

CHAPTER 2 - PROCEDURE

2.1 Experiment Plan

One blast line was installed running generally southeast from ground zero; eight stations, each containing two gages, were located at 0, 100, 200, 400, 800, 1500, 3000, and 6000 feet nominal distance. The ground zero station consisted of two gages suspended at a height of 3 feet above the concrete pad approximately 21 feet from surface zero. Because of uncertainty in the expected overpressure, each of the two gages had different set ranges (Table 2.1). Thus, if the overpressure was higher than expected, the low range gage would be overranged and the higher range gage would record satisfactorily. Similarly, if the overpressures were small, the lower range gage would record the signal even if it fell below the sensitivity of the higher range gage.

TABLE 2.1

Location and Set Ranges of Gages

Station No.	Location (from Surface Zero) Feet	Meters	Expected Overpressure (psi) High Range	Low Range
1	21	6.0	10.0	3.0
2	100	30.5	5.0	1.0
3	200	61.0	2.5	0.5
4	400	122.0	1.0	0.2
5	800	244.0	0.6	0.12
6	1500	457.0	0.35	0.070
7*	3000	914.5	0.15	0.030
8	6000	1829.0	0.075	0.015

*Station 7 was later moved 300 feet further out to avoid unfavorable land forms.

The "as-built" locations of gage stations were:

Elevation (feet)	Range (feet)	Azimuth
6197.45	3.35	
6192.04	99.74	S49°49'57"E
6181.86	199.78	S49°56'56"E
6159.70	397.32	S59°4'40"E
6136.03	800.80	S58°54'28"E
6094.75	1446.81	S57°1'3"E
6236.47	3300.03	S58°59'43"E
6112.82	6000.89	S58°58'10"E

The ground zero gage was suspended with the gage port at 36 inches above the concrete pad. Consequently, it recorded only until the pad was driven into the gage. All other gages were installed in canisters in the ground with the gage port opening into the plane of the ground surface. An area with a radius of about 15 feet was cleared of brush and boulders at each station.

2.2 Instrumentation

Pace P-7 diaphragm-type pressure gages were used. Information was carried through Consolidated System D amplifiers with an 800-cps response and recorded with an Ampex LP-100 magnetic tape recording system. There was only one gage failure other than those which were anticipated at the ground zero stations when either signal cables broke or the suspended gages came in contact with the rising ground surface.

CHAPTER 3 - TEST RESULTS

3.1 Summary of Results

The more sensitive gage at the 200-foot station failed. All other gages gave readable records. The measured overpressures were below the low ranges listed in Table 2.1.

Table 3.1 summarizes the results of the pressure measurements. The headings of columns are identified in Figure 3.1. Additional identification is made in Figure 3.2. I_1 as illustrated in Figure 3.2 includes all impulses from t_a to t_{I_1}.

The pressure records are reproduced in the Appendix. The less sensitive gages always display more noise simply because the signal is a small part of the total set range. Thus, when two gages at the same station are not in agreement, credence should be weighted in favor of the more sensitive gage.

Agreement between the two gages at each station is good in spite of a factor of 5 difference in set ranges.

3.2 Evaluation of Records

Failure of the ground-zero gage at a relatively early time after recording the ground-shock-induced peak was expected. Since measured pressures did not exceed the expected pressures by which the low ranges were set, the maximum signal amplitude of the less sensitive gages was less than one-fifth of the amplitude the less sensitive gages were set to record. Thus, the signal-to-noise ratio is small for records obtained on those gages. Consequently, cross-over times cannot be obtained with the same degree of precision. Similarly, pressure peaks are generally exaggerated by about half the noise amplitude. Impulse, of course, is little affected.

The records from the more sensitive gage at the 400- and 800-foot stations are increasingly noisy after 2 seconds and the noise may be due to ground waves generated by impact of ejecta in the vicinity of the gages.

TABLE 3.1

Summary of Pressure Measurements

Gage	t_a (sec)	P_1 (psi)	t_{P_1} (sec)	P_2 (psi)	t_{P_2} (sec)	I_1 (psi-sec)	t_{I_1} (sec)	P_{-1} (psi)	$t_{P_{-1}}$ (sec)	I_{-1} (psi-sec)	$t_{I_{-1}}$ (sec)	P_3 (psi)	t_{P_3} (sec)	I_2 (psi-sec)	t_{I_2} (sec)	P_{-2} (psi)	$t_{P_{-2}}$ (sec)	I_{-2} (psi-sec)	$t_{I_{-2}}$ (sec)	P_4 (psi)	t_{P_4} (sec)	I_3 (psi-sec)	t_{I_3} (sec)	
GZ-1	0.032	-	-	1.450	0.065	0.0311*	0.079*	-	-	-	-	-	-	-	-	-	-	-						
GZ-2	0.032	-	-	1.359	0.066	0.0303*	0.079*	-	-	-	-	-	-	-	-	-	-	-						
100-1	0.034	-	-	0.8873	0.084	0.1852	0.630	-0.0088	0.639	0.0000	0.653	0.1148	0.981	0.0421	1.512	-	-	-	Gage failed at 1.552 seconds.					
100-2	0.038	-	-	0.8211	0.084	0.1698	0.630	-0.0450	0.639	0.0004	0.660	0.1012	1.103	0.0379**	1.545**	-	-	-	Gage failed at 1.545 seconds.					
200-2	0.045	-	-	0.6408	0.125	0.1158	0.660	-0.1106	0.507	0.0080	1.030	0.1214	1.230	0.0487	1.845	-0.1214	2.063	0.0198	2.200	Gage failed at 2.431 seconds.				
400-1	0.095	0.1310	0.173	0.2435	0.309	0.0638	0.617	-0.0752	0.864	0.0160	1.055	0.1056	1.360	0.0487	1.926	-0.0709	3.064	0.0739	3.684	0.0702	4.226	0.0859	6.315	Gage failed at 6.4 seconds.
400-2	0.093	0.1247	0.173	0.2316	0.310	0.0589	0.612	-0.0802	0.873	0.0168	1.059	0.0980	1.360	0.0429	1.855	-0.0802	3.115	0.0692	3.652	0.0690	4.576	0.0917	6.383	Gage failed at 6.4 seconds.
800-1	0.183	0.0045	0.286	0.1163	0.712	0.0264	0.988	-0.0113	1.046	0.0010	1.353	0.0511	1.785	0.0229	2.295	-0.0410	3.376	0.0428	4.075	0.0281	4.655	0.0231	5.615	Gage failed at 7.2 seconds.
800-2	0.195	0.0081	0.286	0.1213	0.709	0.0277	0.996	-0.0108	1.046	0.0006	1.335	0.0553	1.733	0.0262	2.400	-0.0454	3.146	0.0366	4.000	0.0353	4.569	0.0213	5.646	Gage failed at 7.4 seconds.
1500-1	0.372	0.0096	0.837	0.0464	1.317	0.0140	1.730	-0.0018	1.747	0.0000	2.064	0.0283	2.389	0.0117	2.806	-0.0240	3.863	0.0251	4.708	0.0149	5.254	0.0113	6.192	Gage failed at 7.38 seconds.
1500-2	0.380	0.0114	0.826	0.0513	1.317	0.0148	1.735	-0.0030	1.745	0.0001	2.060	0.0298	2.378	0.0114	2.820	-0.0270	3.788	0.0277	4.637	0.0147	5.409	0.0133	6.136	Gage failed at 7.38 seconds.
3300-1	0.746	0.0025	1.517	0.0204	3.007	0.0053	3.452	-0.0015	3.505	0.0002	3.785	0.0135	4.117	0.0050	4.490	-0.0112	5.434	0.0127	6.425	0.0061	6.919	0.0045	7.695	
3300-2	0.748	0.0032	1.517	0.0186	3.010	0.0053	3.328	-0.0021	3.489	0.00021	3.807	0.0119	4.123	0.0048	4.422	-0.0114	5.612	0.0140	6.525	0.0062	6.996	0.0042	7.755	
6000-1	1.015	0.0015	3.598	0.0087	5.566	0.0032	6.123	-0.0011	6.245	0.0001	6.335	0.0062	6.660	0.0026	7.114	-0.0065	8.089	0.0075	8.995	0.0037	9.418	0.0027	10.355	
6000-2	1.015	0.0021	3.610	0.0088	5.569	0.0036	6.135	-0.0014	6.246	0.0001	6.332	0.0265	6.665	0.0027	7.128	-0.0068	8.114	0.0073	8.995	0.0039	9.416	0.0026	10.395	

-1 - Indicates the more sensitive gage (low range).

-2 - Indicates the less sensitive gage (high range).

*Partial Impulse--Gages failed at 0.079 second.

**Not an accurate value.

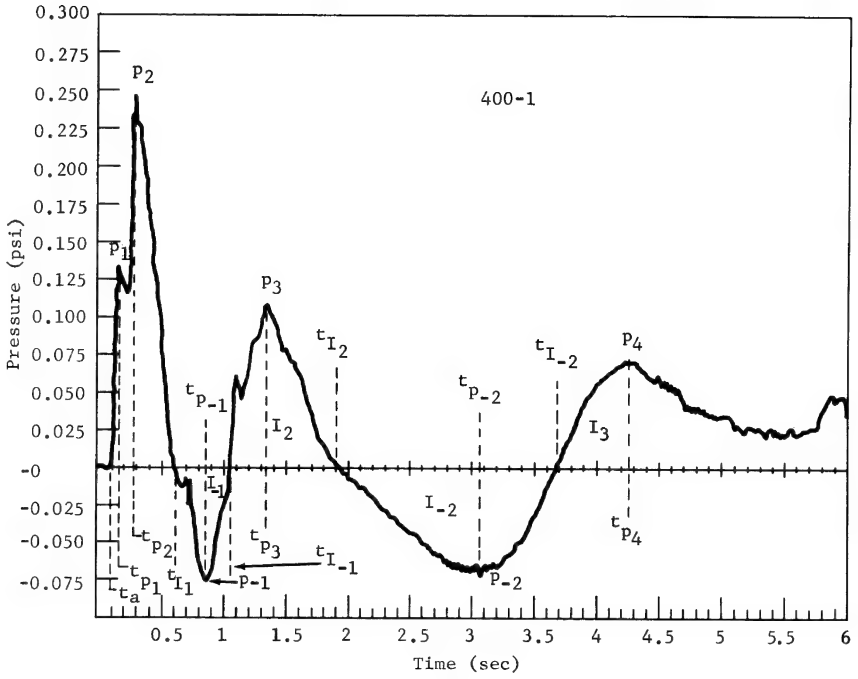

Figure 3.1. Definition of events in Cabriolet pressure records

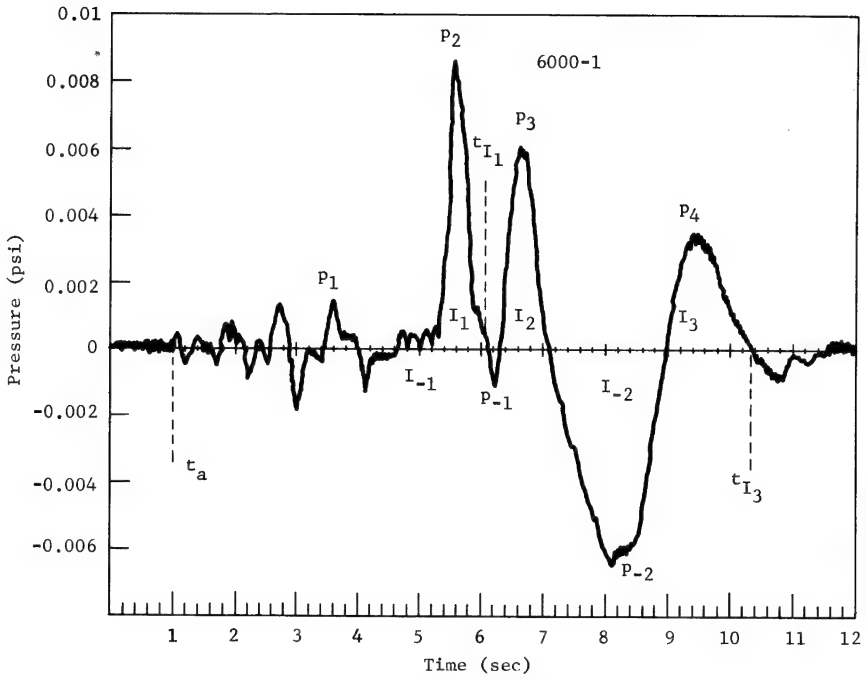

Figure 3.2. Definition of events in Cabriolet pressure records

CHAPTER 4 - DISCUSSION AND INTERPRETATION

4.1 Introduction

Following the pattern of earlier reports this chapter treats the blast wave constituents in a chronological order.

4.2 Ground-Transmitted, Ground-Shock-Induced Pulse

Arrival Times -- The ground-transmitted, ground-shock-induced pulse cannot be separately identified from the air-transmitted, ground-shock-induced pulse at any of the stations. As indicated in the description of pulses in Section 1.3, the two pulses are the same at the epicenter. They are distinguishable primarily by their propagation velocities. The ground-zero (GZ) gage was mounted 3 feet above and 3.35 feet away from GZ. The signal arrives at 32 msec and climbs gradually to a peak at 65 msec. The rise is shown clearly in Figure A.1.

Because of transit time from the concrete pad to the gage the arrival at the ground surface would be nearly 3 msec earlier. The slow rise at the GZ station is in contrast to the clean sharp breakaway at 34 msec seen in the record of Gage 100-1 which was flush-mounted in the ground. There is no ready explanation for the slow rise at the GZ station. The arrival time is consistent with that at the 100-foot station. The arrival at the GZ station indicates an average velocity in the medium of 5828 ft/sec, less than the approximately 7000 ft/sec average velocity for the Palanquin event. It is also less than the 7220 ft/sec (2200 msec) assumed for early Cabriolet calculations.

The computed average velocity takes into account the fact that the epicenter gage was 3 feet above the surface. Using the average velocity at the GZ station, ground shock should arrive at the 100-foot station at 34.3 msec, essentially the 34 msec measured by Gage 100-1. By the same reasoning, anticipated arrival at Gage 200-2 was 45.1 msec but the measured arrival time of 45 msec was admittedly not an accurate arrival time because of noise in the record of this less sensitive gage. Calculated ground shock and measured arrivals at the 400-foot station were 74.6 and 93 to 95 msec, respectively. Based upon relative ground and air shock velocities it is estimated that the ground-shock-induced wave changed from a ground-transmitted wave to an air-transmitted wave at about 375 feet. Thus, the apparent source of the air-transmitted ground-shock induced wave is 375 feet from the epicenter, i.e., the piston had a radius of 375 feet.

Peak Overpressures -- Peak overpressures of this pulse will be discussed with the air-transmitted ground-shock-induced pulse.

4.3 Rayleigh-Wave-Induced Pulse

Arrival Times -- The Rayleigh-wave-induced pulse is identified at the 800-foot station and beyond. It can be identified within the wave train by assuming a velocity of about 3,000 to 3,500 ft/sec or about half the sonic velocity; thus it can be separated from waves arriving earlier at the two most distant stations as shown in Table 4.1.

TABLE 4.1

Velocities Between Stations

	First Wave		Rayleigh Wave	
Distance (ft)	Arrival Times (sec)	Average Velocity Between Stations (ft/sec)	Arrival Times (sec)	Average Velocity Between Stations (ft/sec)
801	0.183	3418	0.183	3418
1447	0.372	4955	0.372	3530
3300	0.746	9959	0.897	3246
6001	1.015		1.729	

The first wave arriving at the two most distant stations is assumed to be refracted from a compressional wave through a deeper high-velocity medium underlying the rhyolite.

The average velocity over the entire range is 6250 ft/sec--slightly higher than the sonic velocity inferred from shock arrival at the ground-zero station. The irregularity in velocity may result from an arrival time derived from arrival of the first observable wave--which may be different from the first observed at a different station.

It is in order to point out that evidence of the Rayleigh wave train can be seen superimposed on the air-transmitted pulses at most stations. One pronounced effect of this superposition is the irregularity it produces in crossover times which are used to define boundaries between individual pulses.

Peak Overpressures -- As is apparent from the records in the Appendix, the maximum amplitude in the Rayleigh wave train is different at each station. Because the Rayleigh wave has a higher velocity than air transmitted waves the number of cycles preceding the air transmitted wave increases as the distance increases. At 800 feet there was only one wave; at 1500 feet there were two, and the second was the larger; at 3300 feet there were three, the second being the larger; and at 6000 feet there are about seven waves, the sixth being the largest. At most stations the later portions of the Rayleigh wave train can be seen superimposed on the air-transmitted pulse. The values listed in Table 3.1 are for the maximum positive amplitude in the train regardless of where it occurs.

4.4 Air-Transmitted, Ground-Shock-Induced Peak Overpressure

Arrival Time -- The time of peak overpressure of the air-transmitted ground-shock-induced pulse (t_{p_2} of Table 3.1) indicates an average propagation velocity between stations at 400 feet and 6000 feet of 1065 ft/sec. The wind at shot time over the region where the blast wave would be affected by wind ranged from 17 to 34 ft/sec at 160 degrees. The blast line azimuth ranged between 140 and 149 degrees. Thus, wind could account for an apparent sonic velocity of from 1057 to 1074 ft/sec. Based on ambient calculations of 802 mb* and 1.6 C* the ambient sonic velocity should have been 1091 ft/sec.

Peak Overpressure -- Peak air-transmitted, ground-shock-induced overpressures are shown in Figure 4.1. The gages from 400 to 6000 feet indicate an attenuation rate** of $R^{-1.23}$--close to the attenuation rates of IBM-M extrapolated to these lower pressures. None of the other peaks exceeded the air-transmitted ground-shock-induced peaks.

Impulse -- In determining impulse (I_1) of air-transmitted ground-shock-induced pulse all portions of the record from the arrival of the first signal to the crossover following the pulse have been included (Figure 4.2). This means that for records obtained from the distant station where there was a significant Rayleigh-wave-induced pulse, any impulse attributed to that pulse was included. The error introduced should be small since the negative and positive portions of the Rayleigh train approximately cancel each other. The first positive phase impulse attenuates with distance about as $R^{-1.10}$.

4.5 First Negative Phase

The first negative phase which separates the ground-shock-induced pulse from the pulse from venting gases was too irregular for reasonable analysis. At each station the values were small.

4.6 Gas Venting Pulse

Arrival Time -- Arrival times of the overpressure peaks indicate an average velocity of 1068 ft/sec from the 200- to the 6000-foot station. This agrees quite well with the average velocity of the ground-shock-induced peaks. The pulse was easily identified in contrast to similar pulses on some of the earlier events. The arrival times of peaks from venting gases from all but the three closest stations when extrapolated back to GZ indicate a source (i.e., venting) at about 1 second. Motion pictures show first venting at 800 ± 25 msec. The agreement is quite good since arrival of the gas venting pulse is 200 to 400 msec prior to the arrival of peak values.

---

*Based on values extrapolated from the Cabriolet Control Point to GZ.[11]

**Attenuation rates in this chapter are based on a first-order least square fit to measure values where values from the more sensitive gages have been weighted five times those of the less sensitive gages because of the factor of 5 difference in set ranges.

Peak Overpressures -- Peak pressures were low at both the 100- and 200-foot stations as evidenced in Figure 4.3 and by the records in the Appendix. It is hypothesized that the low readings are a result of shielding provided by the edge of the mound at the time the venting gases erupt. The peak overpressure attenuates with distance at approximately $R^{-1.02}$ from 400 to 6000 feet.

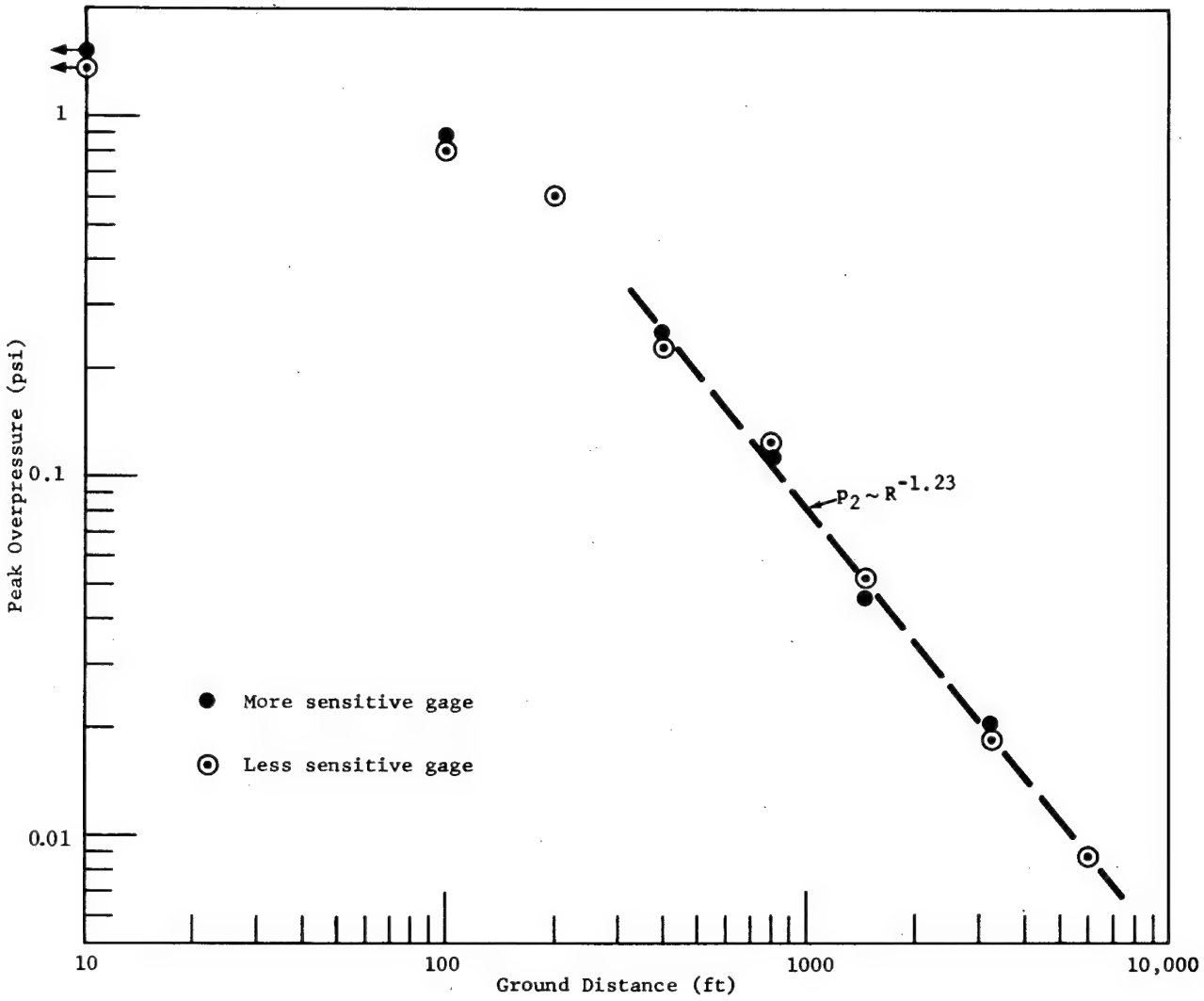

Figure 4.1 Ground-shock-induced peaks (p_2)

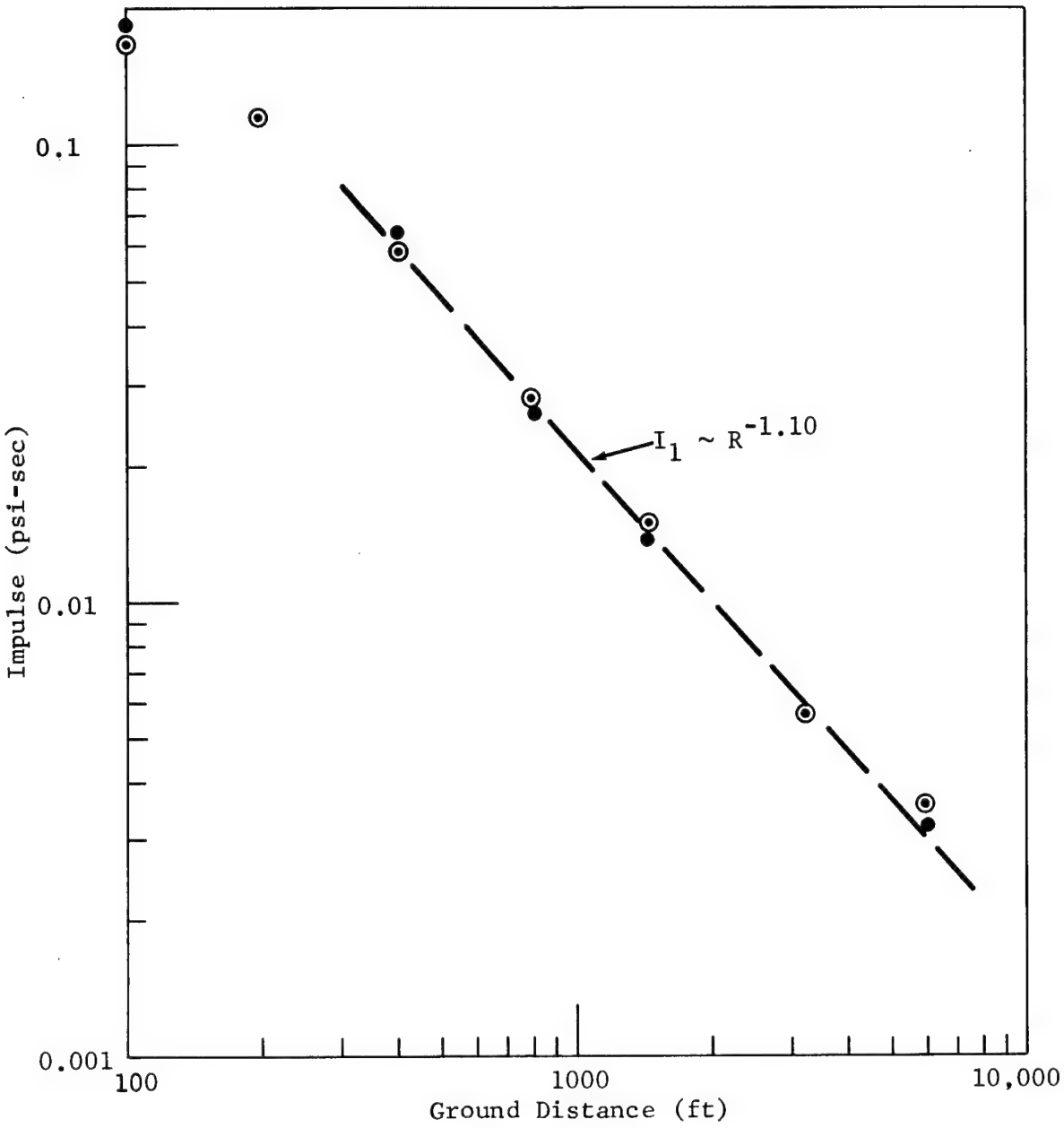

Figure 4.2 Ground-shock-induced impulse

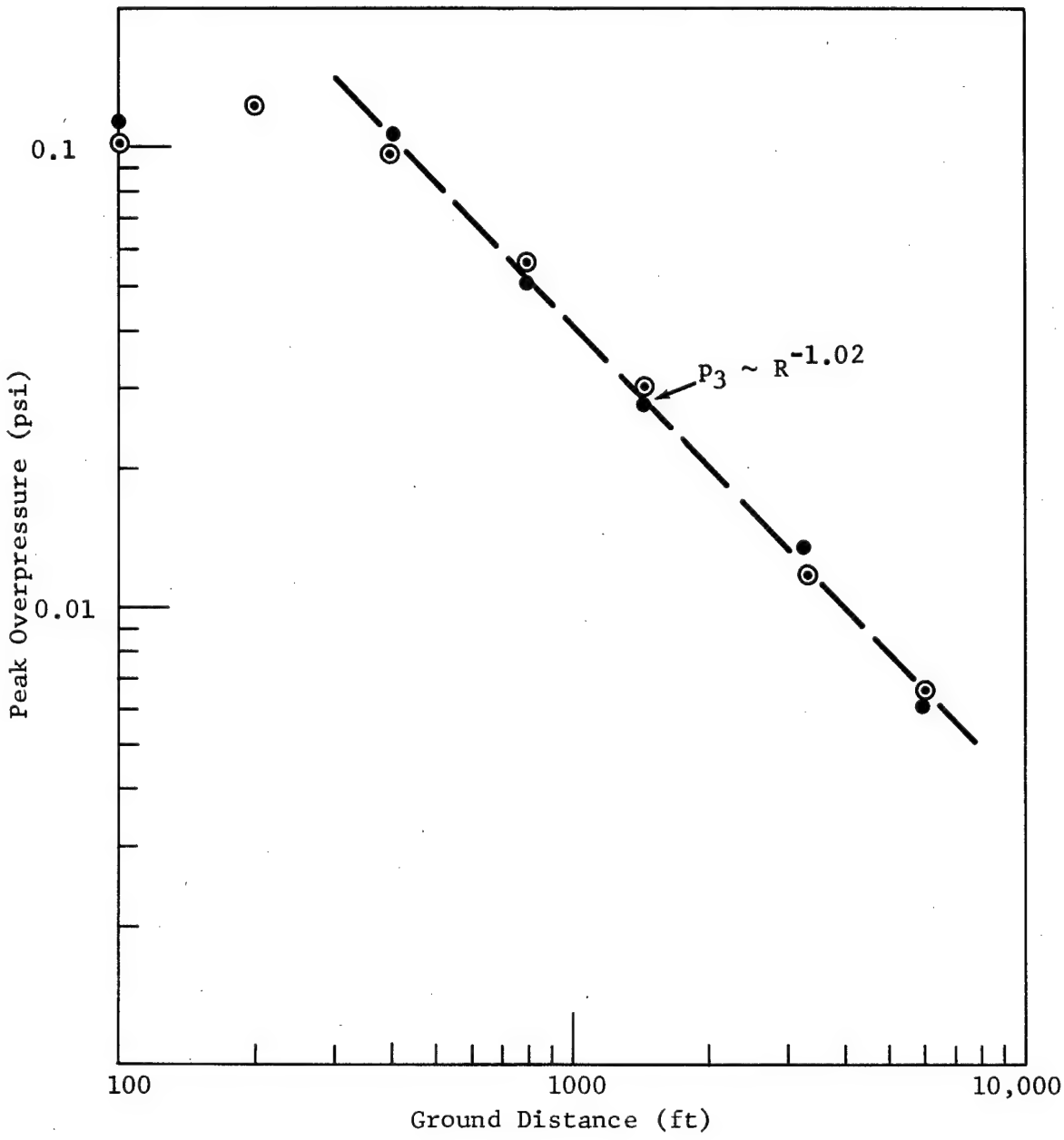

Figure 4.3 Gas venting peak (p_3)

Impulse -- The impulse (Figure 4.4) also indicates possible diffraction of the blast wave over the edge of the dome from which the gases vented. Between 400 and 6000 feet, the impulse attenuated at $R^{-1.07}$.

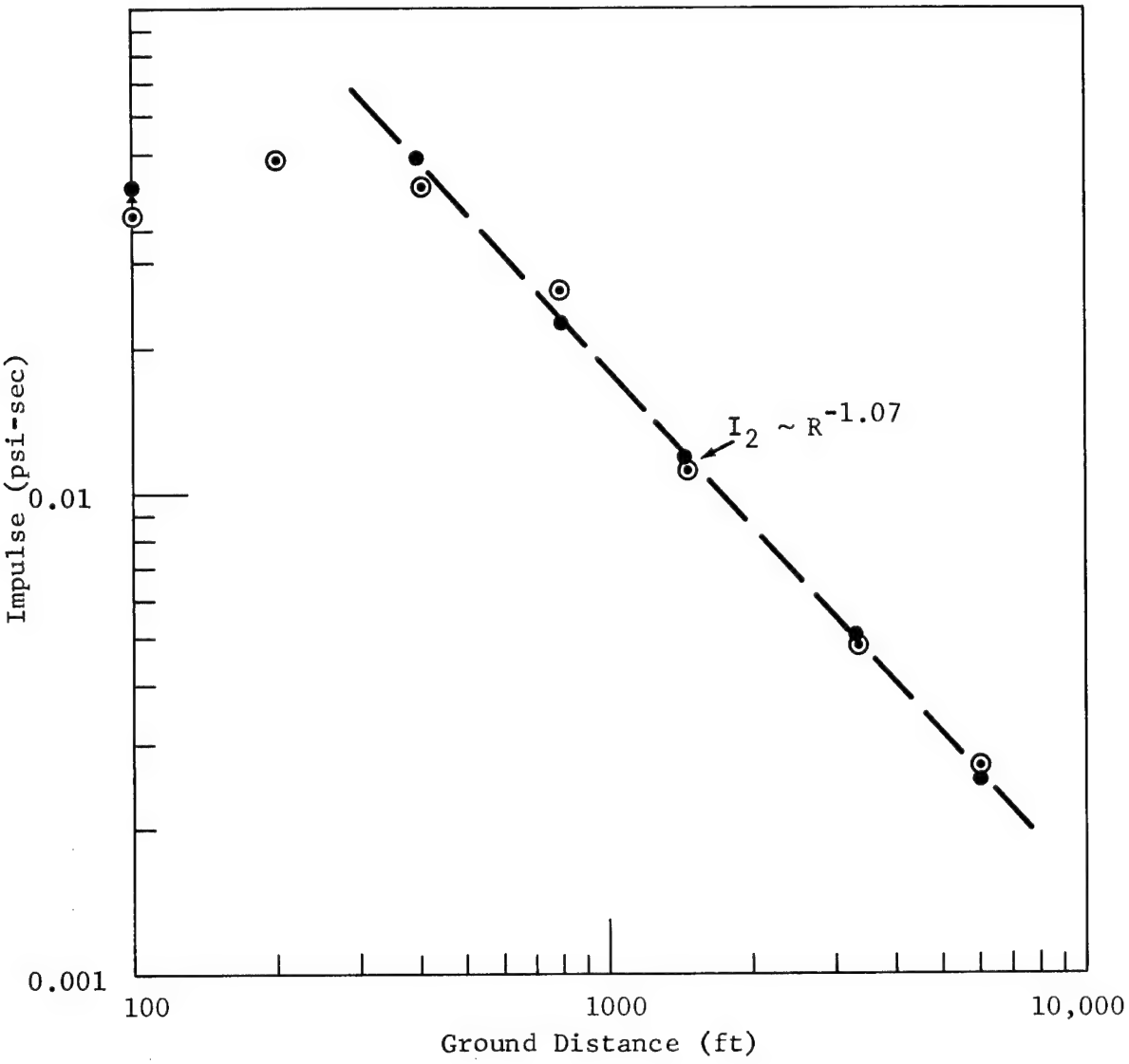

Figure 4.4 Gas venting impulse (I_2)

4.7 Second Negative Phase

The second negative phase is a good pulse to use in evaluating the quality of the instrumentation. The pulse is a broad one with few high-frequency components, and hence little affected by acoustic damping should such damping be inherent in the gage. Since the wave attenuates at a uniform rate, the consistency of the values obtained from one station to the next is a very good measure of the consistency of calibration of the gages. Where an individual measurement deviates

from a pressure-distance curve the deviation often indicates an error in calibration. If a similar deviation appears also on a positive impulse, a calibration error is virtually substantiated. If both positive and negative pulses are in error but in opposite directions, a base line shift is indicated. The base line shift can, of course, be corrected after the fact as has been done in the case of the record from Gage 3300-2. The uniform wave permits a good measure attenuation rate which was found to be $R^{-0.89}$ (Figure 4.5) for peak negative pressure and $R^{-0.84}$ for negative impulse.

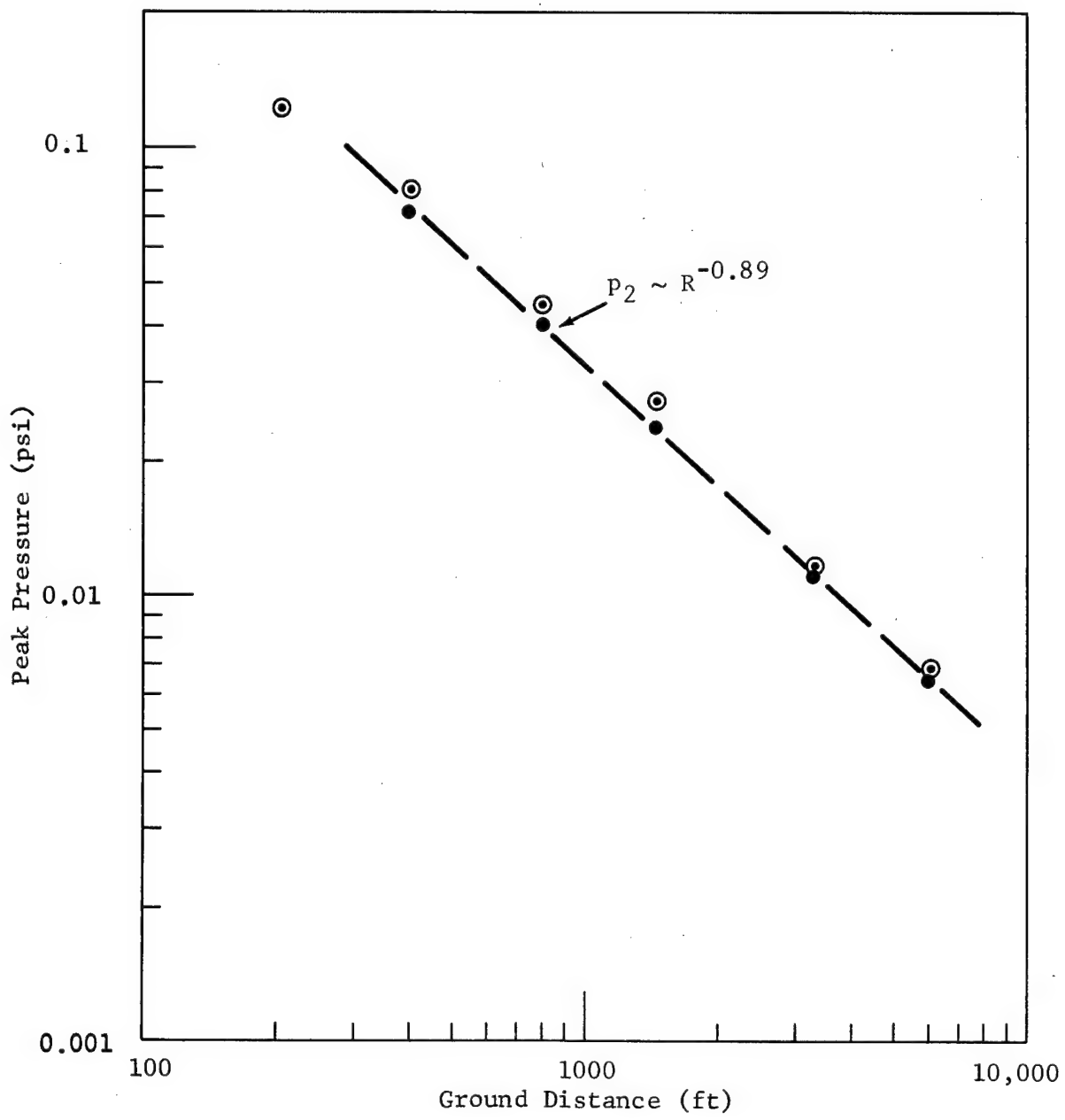

Figure 4.5 Second negative peak (p_{-2})

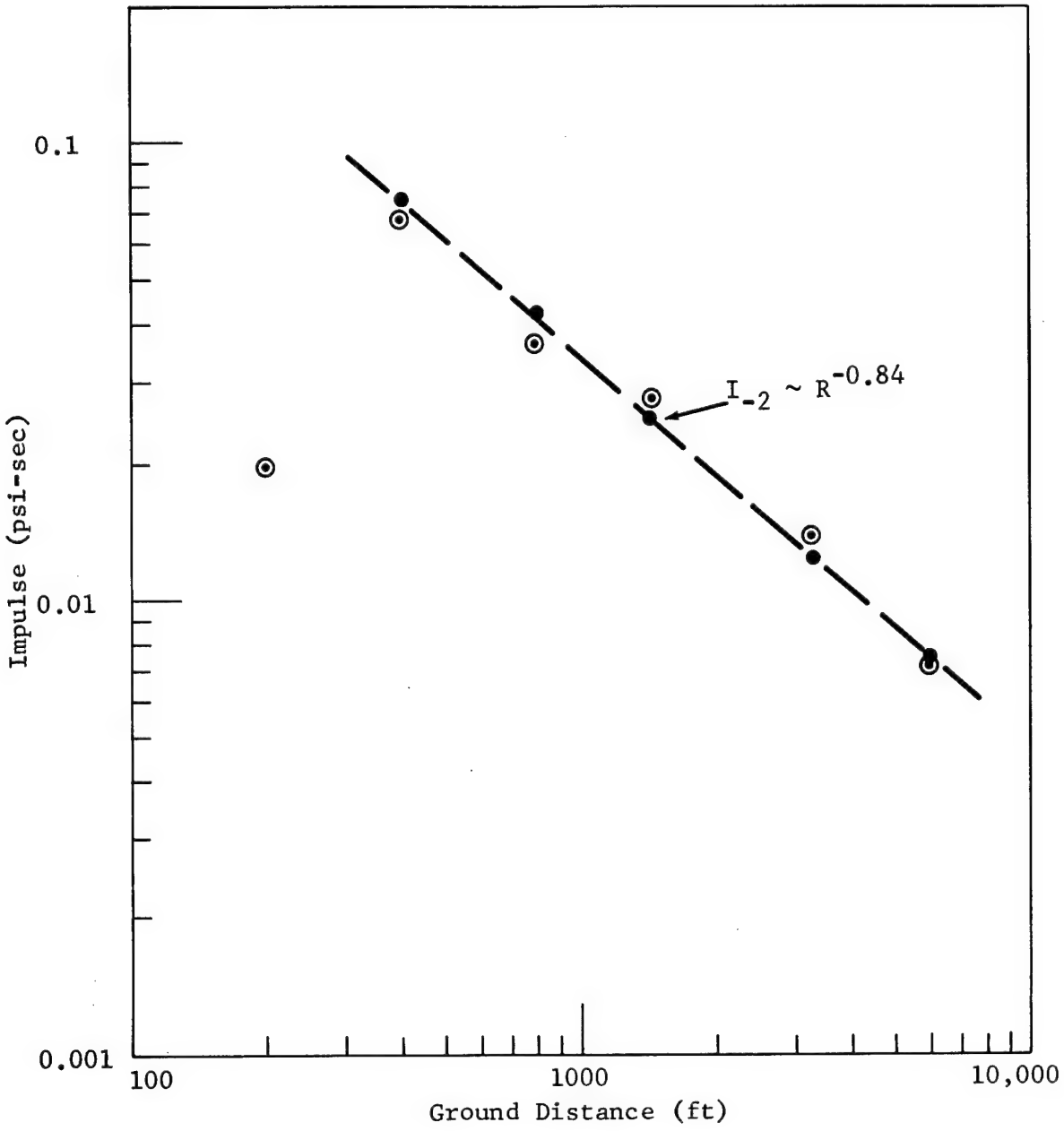

Figure 4.6 Second negative impulse (I_{-2})

4.8 Fourth Positive Phase

This pulse was identified on earlier events as a restoration pulse brought about when the inrushing air of the preceding negative pulse overshoots and moves outward again in its restoration to ambient conditions.

Peak Overpressure -- Because of failure of the close-in gages from ground motion, no fourth positive phase is seen closer than 400 feet. The relatively broad pulse attenuates at about $R^{-1.08}$.

Impulse -- The impulse of the fourth positive pulse shows remarkable uniformity from one station to another considering differences in recovery to ambient and differences in times at which records were terminated by debris destroying gages or cutting cables of the closer gages.

4.9 Comparison with Past Explosions

Figures 4.8 and 4.9 compare the results of Cabriolet with comparable measurements for other nuclear detonations and corollary chemical explosive events. The comparison is made at a scaled ground range of 5 $ft/lb^{1/3}$.* The peak ground-shock-induced overpressures (Figure 4.8) show that the peak overpressures in NTS alluvium[12-16] are reasonably uniform and in good agreement with those for the Albuquerque alluvium.[17] The peak overpressures from chemical explosions in basalt[18,19] indicate a higher overpressure, as would be expected from the better shock transmission in the denser medium. Ground-shock-induced peak overpressures from the Pre-Schooner II[19] event were particularly large because of an unusually sharp high spike on the ground-shock-induced pulse.

No ground-shock-induced pulses were observed on Teapot ESS[20] or Sedan.[21] The ground-shock-induced pulse was the dominant pulse on the two nuclear events in basalt and those in rhyolite. Note that the results of Danny Boy,[5] Sulky,[7] and Cabriolet agree reasonably well with those obtained for chemical explosions in soil. The peak pressures fall short of those seen for chemical explosions in rock.

For explosions in air, it has been observed that pressure-distance relationships from nuclear explosions can be made to agree with those from chemical explosions (TNT) if the nuclear explosion is considered to have the blast equivalent of one million, rather than two million, pounds of TNT per kiloton. If a similar argument is applied to Danny Boy, Sulky, and Palanquin, then each shot would be at a deeper scaled burial depth and would more nearly agree with the peak ground-shock-induced overpressure from the chemical explosions in basalt. This is evidenced by the fact that the open data points in Figure 4.8 for nuclear shots in rock fall closer to the HE basalt curve when scaled on the basis of one million pounds per kiloton. Note that Cabriolet

*Because attenuation rates vary slightly from shot to shot comparisons at other scaled distances may yield slightly different results.

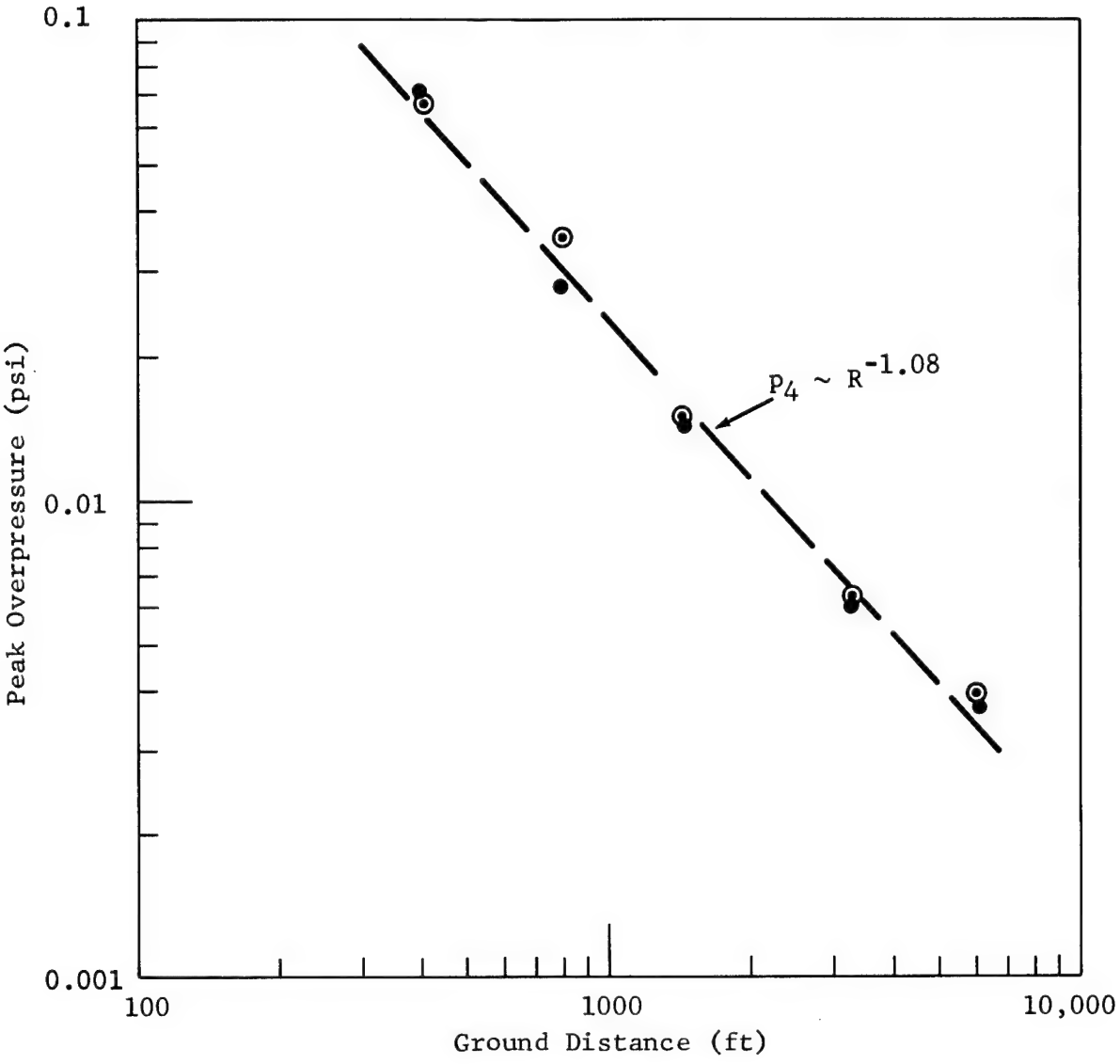

Figure 4.7 Fourth positive peak overpressure (p_4)

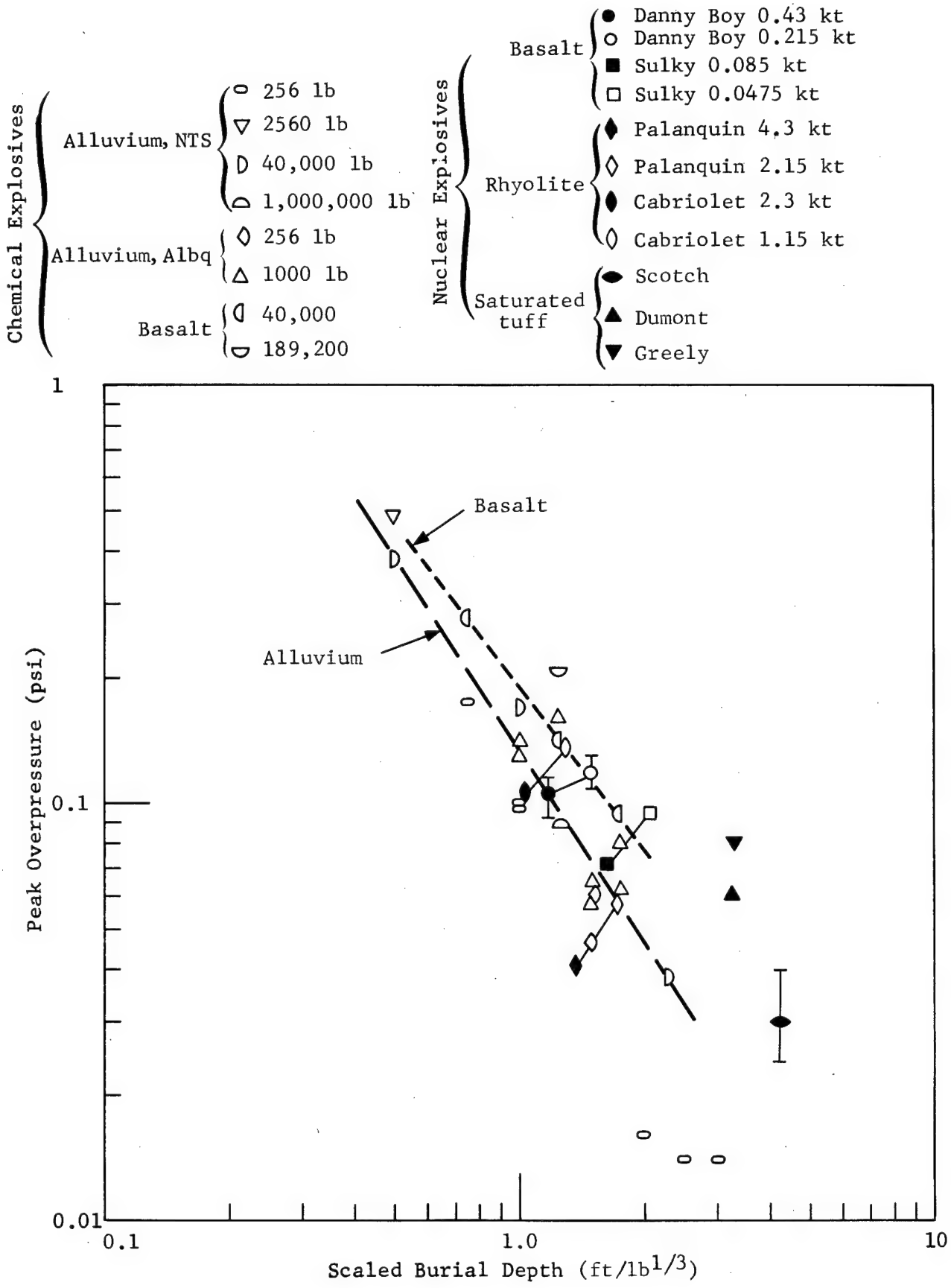

Figure 4.8 Peak ground-shock-induced overpressure at 5 ft/lb$^{1/3}$

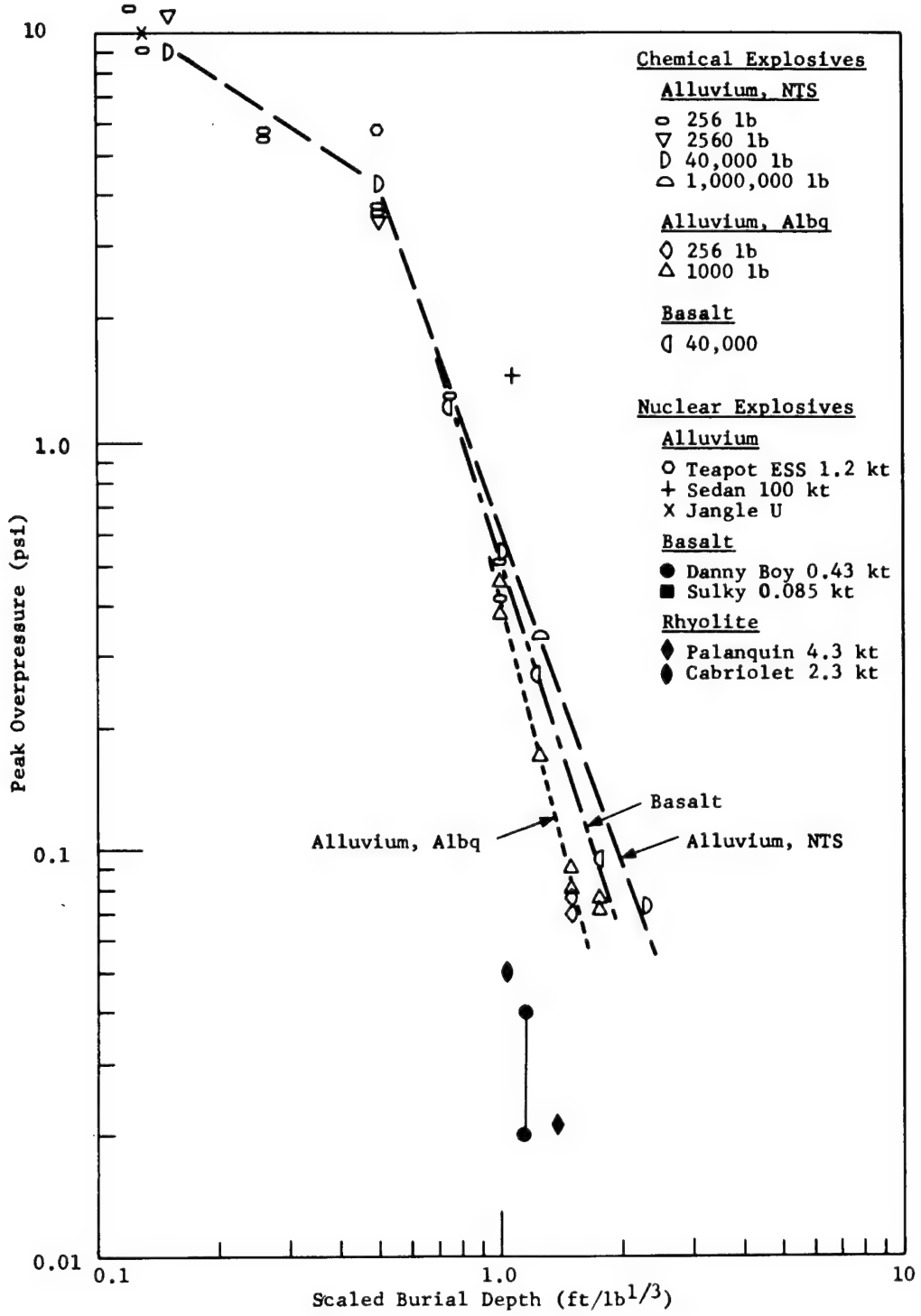

Figure 4.9 Peak overpressure from venting gases at 5 $ft/lb^{1/3}$

agrees rather precisely. This is the first time there has been sufficient evidence to suggest that a blast equivalence of the type found for free-air burst may apply also for buried explosions.

Note in the figure that Palanquin value falls far below the others. It was on the basis of a comparison such as this that an apparent blast yield for the Palanquin event was deduced from the overpressure measurements.

The peak overpressures from venting gases tell an entirely different story (Figure 4.9). Here the overpressure peaks from chemical explosions in NTS alluvium are slightly higher than those from similar explosions in basalt. Results from detonations in the Albuquerque alluvium fall below those in both the other materials.

The nuclear shots are completely inconsistent. Two shots in alluvium, Teapot ESS and Sedan, had only a pulse from venting gases, each with peaks considerably larger than any of those expected from chemical explosions at comparable burial depths. Until a better explanation is forthcoming, this large pulse is attributed to vaporization of moisture in the soil.

Jangle U^{22} gave results comparable with pressures from chemical explosions--not surprising since the relatively shallower burial depth would make medium effects less pronounced.

The results from nuclear shots in rock, in contrast to those from shots in soil, show a very weak pulse from venting gases. The Sulky event gave overpressures which were equal to or less than the ambient pressure. Pressures from venting gases for Danny Boy, Palanquin, and Cabriolet appear to form a consistent pattern--all much lower than those from chemical explosions. These lower pressures are attributed first to the small amount of gas produced because of the lower moisture content of the rock media, and second to the fact that in some cases the pulse from venting gases appears superimposed on a negative phase following the ground-shock-induced pulse, resulting in somewhat decreased peak values.

4.10 Comparison of Air Blast from Palanquin and Cabriolet

The waveforms of air blast of Palanquin and Cabriolet are quite different as evidenced by Figure 4.10 which reproduces records from gages at nearly the same distance. The differences are obvious from the figure and point up the variations which can occur from relatively similar events. Table 4.2 compares the emplacement conditions for the two shots.

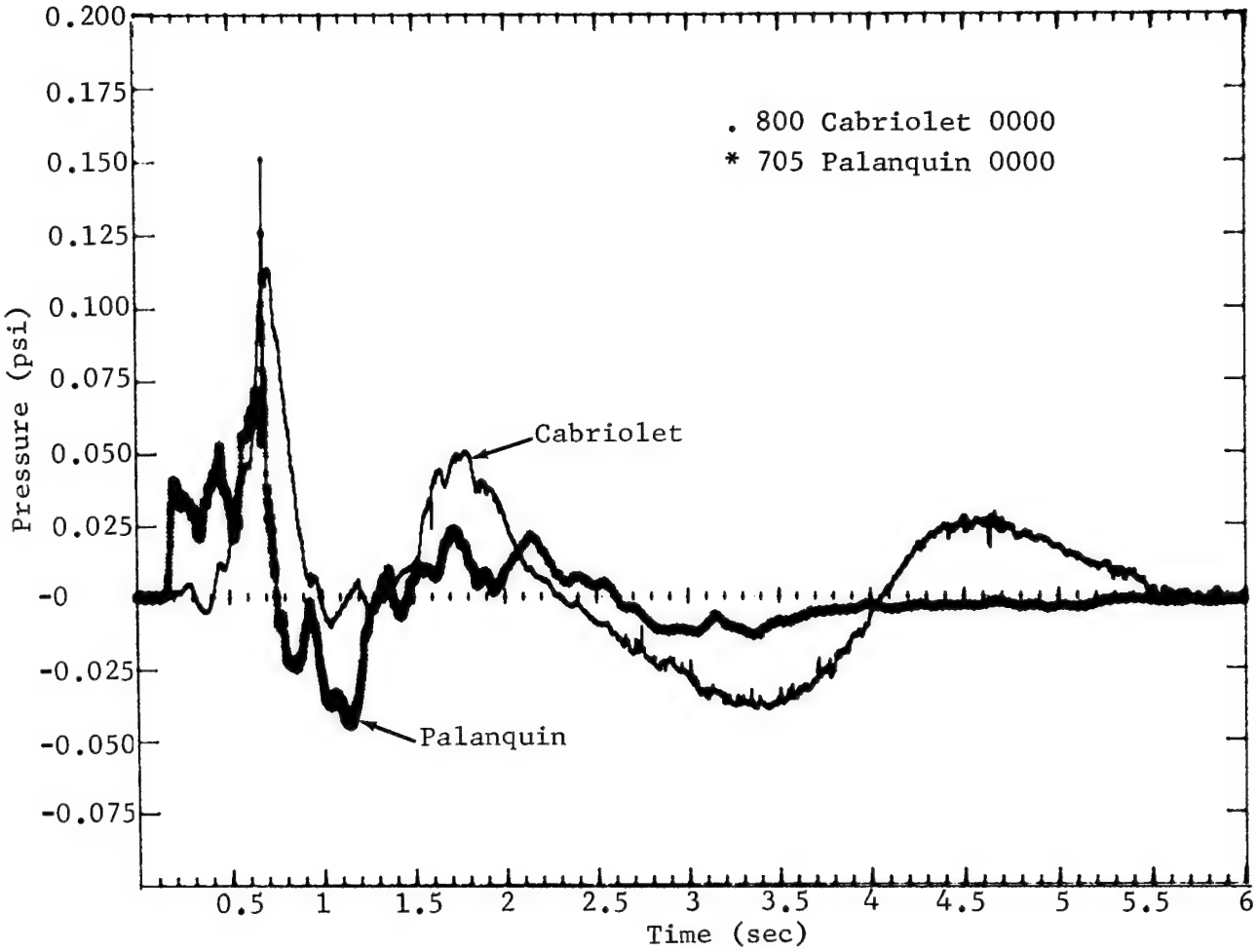

Figure 4.10 Air blast waveforms from Palanquin and Cabriolet

TABLE 4.2

Comparison of Cabriolet and Palanquin

Shot	Yield (kt)	Burial Depth (ft)	Scaled Burial Depth ft/lb$^{1/3}$*	Scaled Burial Depth ft/lb$^{1/3}$**	Scaled Distance to Gages ft/lb$^{1/3}$*	Scaled Distance to Gages ft/lb$^{1/3}$**
Cabriolet	2.3	170.75	1.026	1.294	4.81	6.06
Palanquin	4.3	280	1.367	1.721	3.44	4.34

*Assuming 1 kiloton is equivalent to two million pounds of TNT.

**Assuming 1 kiloton is equivalent to one million pounds of TNT.

The medium was essentially the same for both events. Venting of Palanquin was observed to be atypical[9] and possibly could account for the smaller amplitude and longer duration of the venting pulse. If the mechanism of the restoration pulse (p_4) were better understood its absence from the Palanquin waveform might also be found to be related to the atypical venting.

Even though the venting was atypical, the ground-shock-induced pulses of the two events should be comparable. On the basis of actual distance the peak overpressures from Palanquin were less than those from Cabriolet, as should be expected in view of the relatively deeper depth of Palanquin.

4.11 Shape of the Front of the Ground-Shock-Induced Pulse

In Section 4.2 it was noted that at 375 feet from ground zero the ground-shock-induced pulse ceased propagating as a ground-transmitted signal and began as an air-transmitted signal. The change occured at 75 msec. The peak overpressure at the time of the change was about 0.28 psi (Figure 4.1). From the information at hand there is no means of estimating accurately the peak overpressure 51 feet above the ground surface or the pressure gradient from that point along the surface of the pulse to the intersection with the ground where the overpressure is 0.28 psi. (Figure 4.11 illustrates the geometry of the ground-shock-induced pulse.)

At the present time little is known of source strength and geometry of blast from buried explosions as it propagates above the ground. Some information can be inferred from the data obtained on Cabriolet.

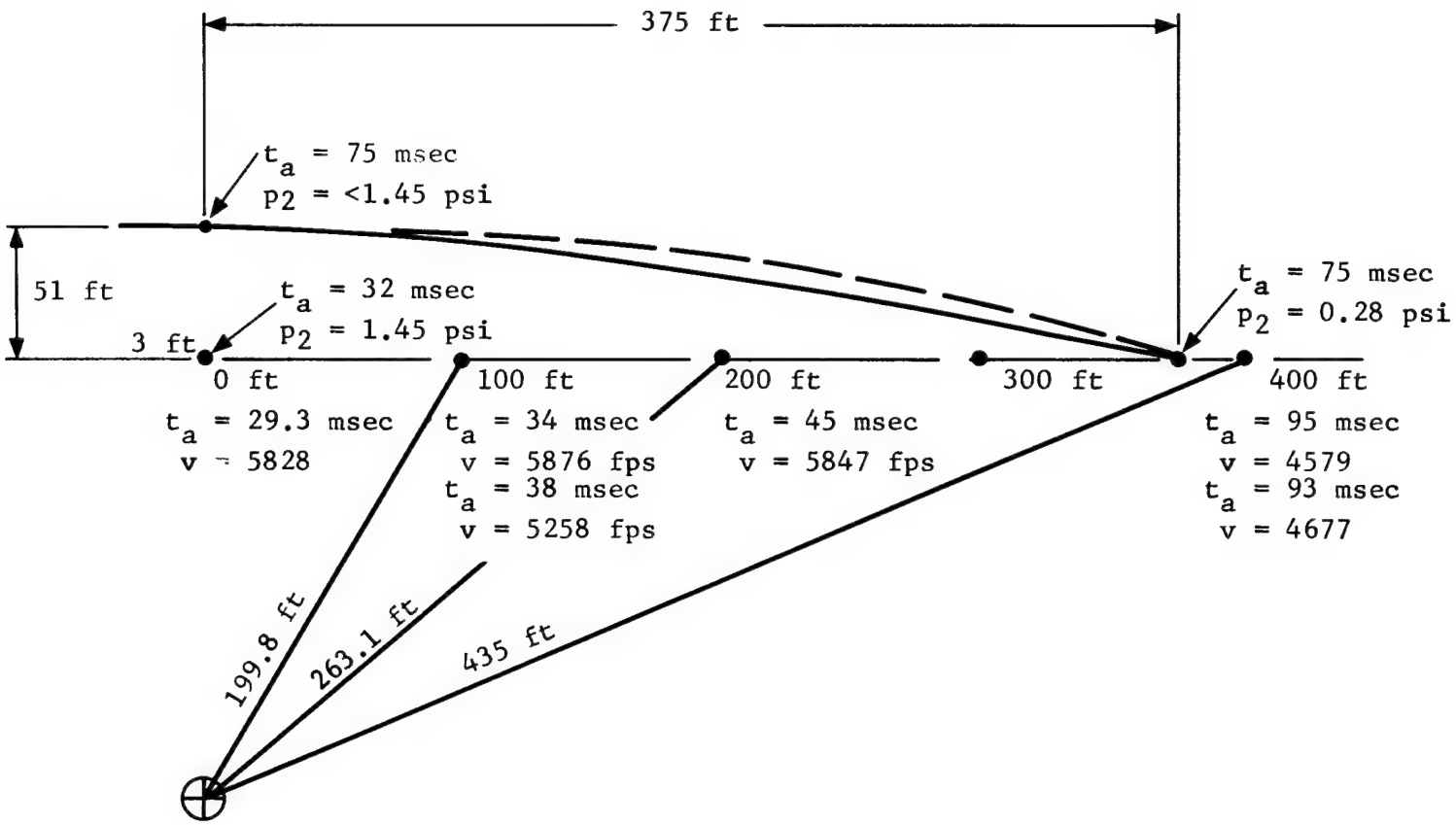

Figure 4.11 Geometry of ground-shock-induced pulse

CHAPTER 5 - SUMMARY AND CONCLUSIONS

On the Cabriolet event overpressure as a function of time was successfully measured by 15 of 16 gages installed. Records from 14 of the 15 gages were among the best produced for any nuclear event to date. As expected, the ground-zero gage was destroyed at an early time by the ground motion. Other close gages stopped recording at times that increased as the distance from ground zero increased. Presumably these gages or their cables were destroyed by falling debris after most of the signals had been obtained.

Based on propagation velocities of the air-transmitted and ground-transmitted, ground-shock-induced pulses, it was deduced that the ground-transmitted pulse became an air-transmitted pulse at 375 feet from the epicenter at about 75 milliseconds.

Rayleigh wave induced pulses were observable at all stations beyond 400 feet. The air-transmitted, ground-shock-induced overpressure constituted the largest overpressure produced by the Cabriolet event.

The venting gas pulse was smaller than the air-transmitted, ground-shock-induced pulse and was especially small at the 100- and 200-foot stations, presumably because of diffraction of the venting gas pulse down from the top surface of the mound through which venting occurred.

A comparison was made of the results of Cabriolet air blast measurements with available data from other nuclear explosions and from the more significant chemical explosions. The results of Cabriolet compare favorably with those of Danny Boy and Sulky. The results of these three events were consistent in that they show a very small pulse from venting gases.

The ground-shock-induced pulse, when used for a comparison between HE and NE, suggests that the air blast from a 1-kiloton nuclear explosion is comparable to that from an HE explosion of only one million pounds. This is the first indication that the relationship between HE and NE which applies to above ground air blast may extend to air blast from buried explosions.

A direct comparison of two gages at about the same actual distance from the explosions indicates both qualitative and quantitative differences between Palanquin and Cabriolet. The quantitative differences are mainly due to differences in burial depth whereas the qualitative differences are probably due to the atypical venting observable on the Palanquin event.

REFERENCES

1. Vortman, L. J., et. al., 20-Ton and 1/2-Ton High Explosive Cratering Experiments in Basalt Rock, Project Buckboard, SC-4675(RR), Sandia Corporation, Albuquerque, New Mexico, November 1960.

2. Vortman, L. J., et. al., 20-Ton HE Cratering Experiment in Desert Alluvium, Project Stagecoach, SC-4596(RR), Sandia Corporation, Albuquerque, New Mexico, January 1962.

3. Perret, W. R., et. al., Project Scooter Final Report, SC-4602(RR), Sandia Corporation, Albuquerque, New Mexico, October 1963.

4. Nordyke, M. D., and Wray, W. R., Preliminary Summary Report, Project Danny Boy, UCRL-6999, Lawrence Radiation Laboratory, Livermore, California, July 1962.

5. Vortman, L. J., Close-In Air Blast from a Nuclear Detonation in Basalt, Project Danny Boy, WT-1810, Sandia Corporation, Albuquerque, New Mexico, September 15, 1962.

6. Vortman, L. J., Close-In Air Blast from a Row Charge in Basalt, Project Dugout, Final Report, PNE-608F, Sandia Corporation, Albuquerque, New Mexico, August 4, 1965.

7. Vortman, L. J., Close-In Air Blast from a Relatively Deep Low-Yield Nuclear Detonation in Basalt, Project Sulky, Final Report, PNE-711F, Sandia Corporation, Albuquerque, New Mexico, to be published.

8. Vortman, L. J., Close-In Air Blast from a Cratering Nuclear Detonation in Rhyolite, Final Report, PNE-902F, Sandia Corporation, Albuquerque, New Mexico, to be published.

9. Videon, F. F., Studies of the Apparent Crater, Project Palanquin, Nuclear Cratering Group, Livermore, California, July 1966.

10. Cabriolet Preshot Analysis, UCRL-14648, Lawrence Radiation Laboratory, Livermore, California, January 20, 1966 (SRD).

11. Private Communication with Don Montan, Lawrence Radiation Laboratory, Livermore, California.

12. Doll, E. B., and Salmon, V., Scaled HE Tests--Operation Jangle, WT-377, Stanford Research Institute, Menlo Park, California.

13. Sachs, D. C., and Swift, L. M., Small Explosion Tests, Project Mole, Vol. I and II, AFSWP-291, Stanford Research Institute, Menlo Park, California.

14. Murphey, B. F., Air Pressure Versus Depth of Burst, SCTM-42-59(51), Sandia Corporation, Albuquerque, New Mexico, February 20, 1959.

REFERENCES (Cont)

15. Vortman, L. J., et. al., 20-Ton HE Cratering Experiment in Desert Alluvium, Project Stagecoach, SC-4596(RR), Sandia Corporation, Albuquerque, New Mexico, January 1962.

16. Perret, W. R., et. al., Project Scooter, Final Report, SC-4602(RR), Sandia Corporation, Albuquerque, New Mexico, October 1963.

17. Unreported data from the CAPSA Series, Sandia Corporation, Albuquerque, New Mexico.

18. Vortman, L. J., et. al., 20-Ton and 1/2-Ton High Explosive Cratering Experiments in Basalt Rock, Project Buckboard, SC-4675(RR), Sandia Corporation, Albuquerque, New Mexico, November 1960.

19. Reed, J. W., and Vortman, L. J., Air Blast Measurements--Pre-Schooner II, PNE-512F, Sandia Corporation, Albuquerque, New Mexico, to be published.

20. Sachs, D. L., and Sachs, L. M., Underground Explosion Effects, WT-1106, Stanford Research Institute, Menlo Park, California.

21. Vortman, L. J., Close-In Air Blast from a Nuclear Event in NTS Desert Alluvium, Project Sedan, PNE-211F, Sandia Corporation, Albuquerque, New Mexico, October 2, 1964.

22. Bishop, J. A., and Lowance, F. E., Cratering Phenomena, Operation Jangle, WT-375, U. S. Naval Civil Engineering Research Evaluation Laboratory, Pt. Hueneme, California, May 1952.

APPENDIX

Pressure-Time Records

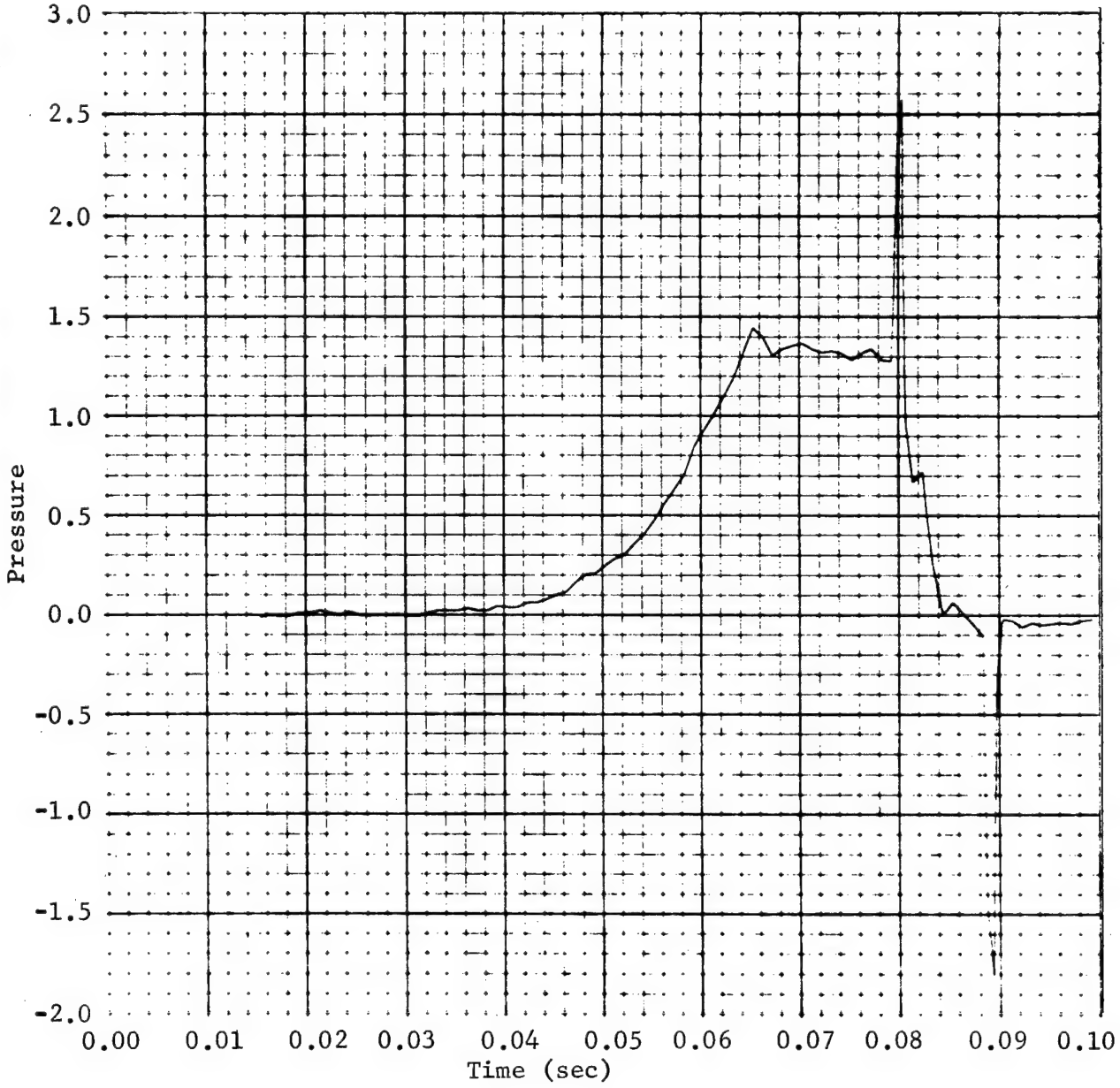
3.0
2.5
2.0
1.5
1.0
0.5
0.0
-0.5
-1.0
-1.5
-2.0
Pressure
0.00
0.01
0.02
0.03
0.04
0.05
0.06
0.07
0.08
0.09
0.10
Time (sec)

Figure A.1

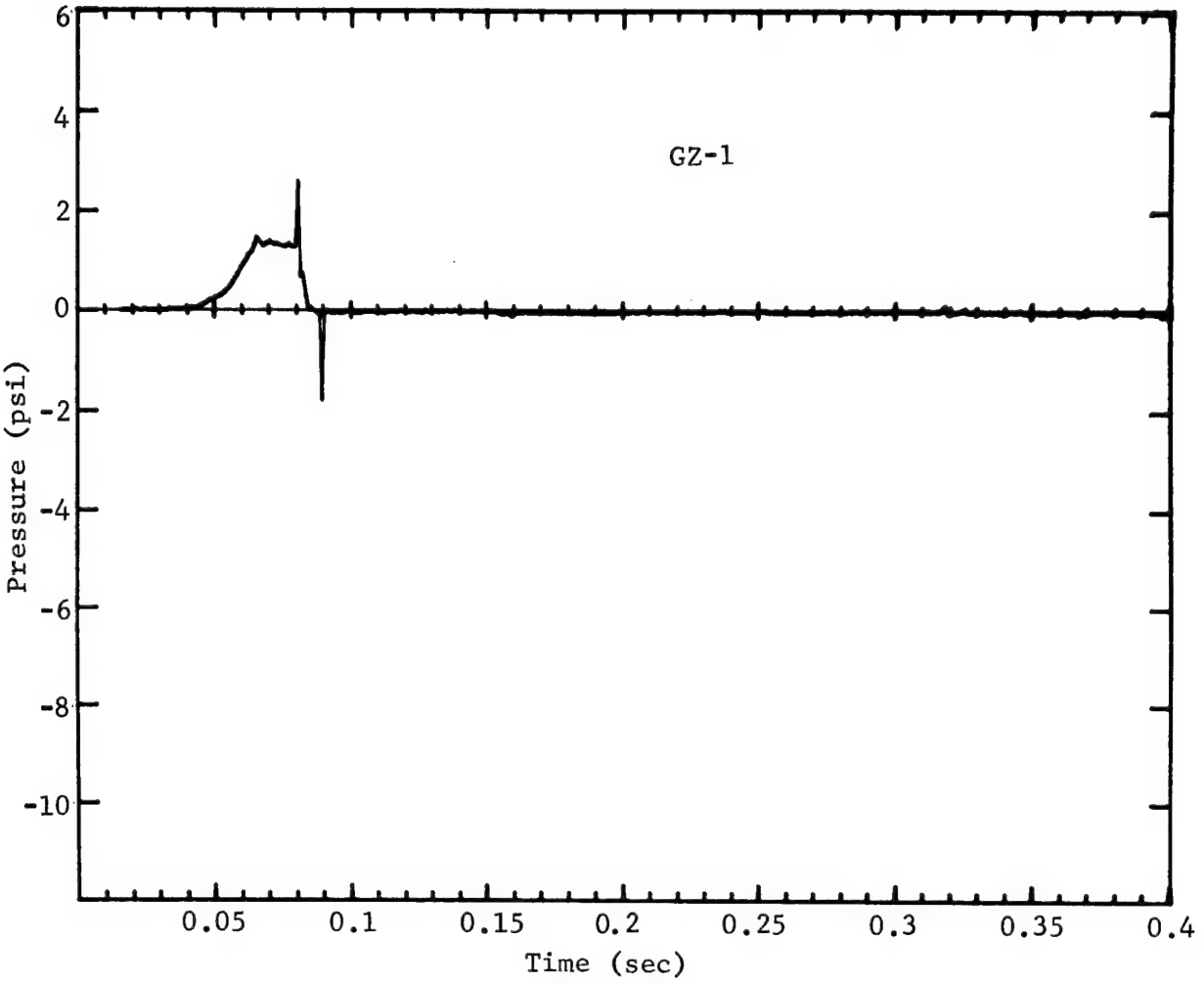
GZ-1
Pressure (psi)
6
4
2
0
-2
-4
-6
-8
-10
0.05
0.1
0.15
0.2
0.25
0.3
0.35
0.4
Time (sec)

Figure A.2

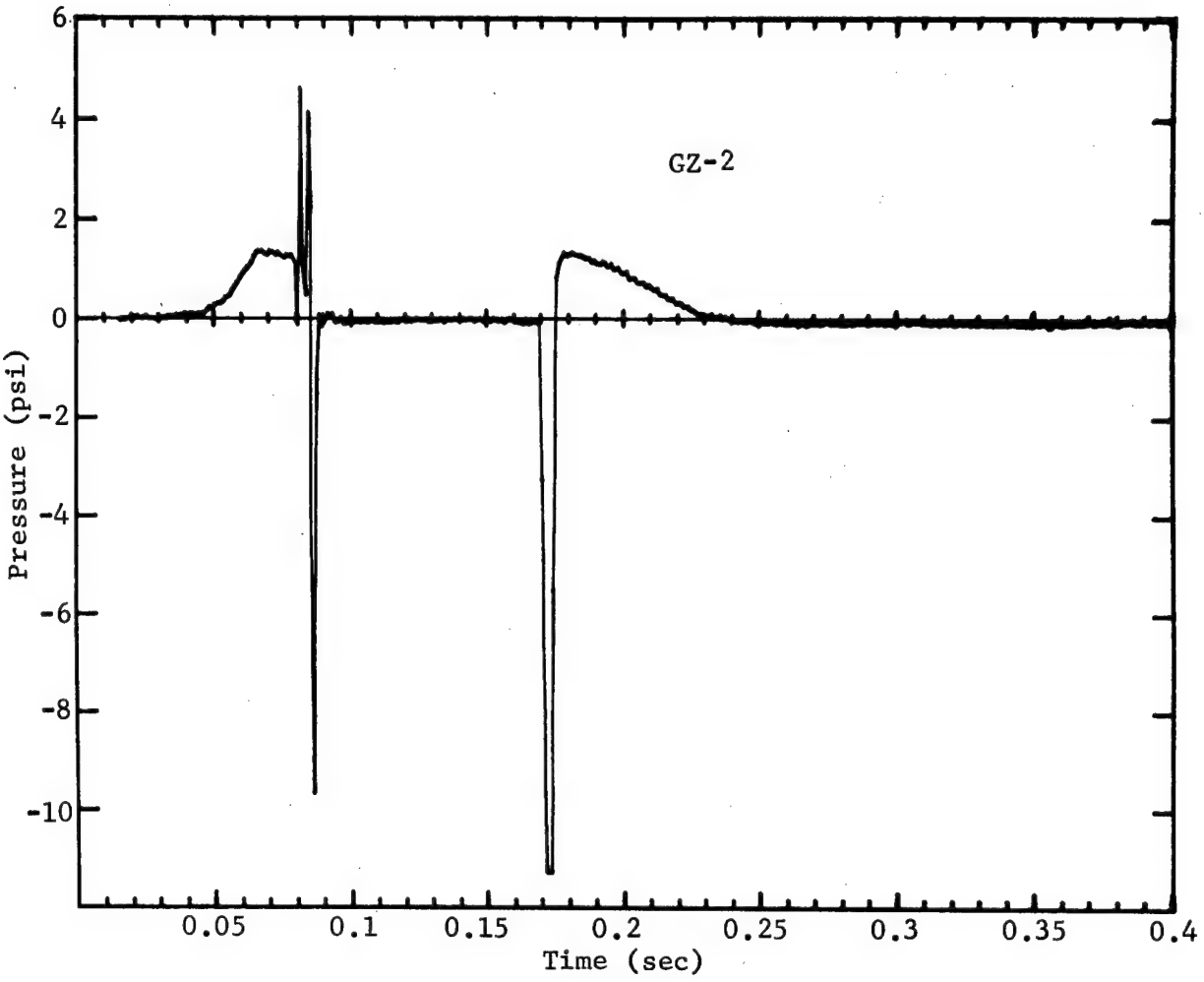
GZ-2
Pressure (psi)
6
4
2
0
-2
-4
-6
-8
-10
0.05
0.1
0.15
0.2
0.25
0.3
0.35
0.4
Time (sec)

Figure A.3

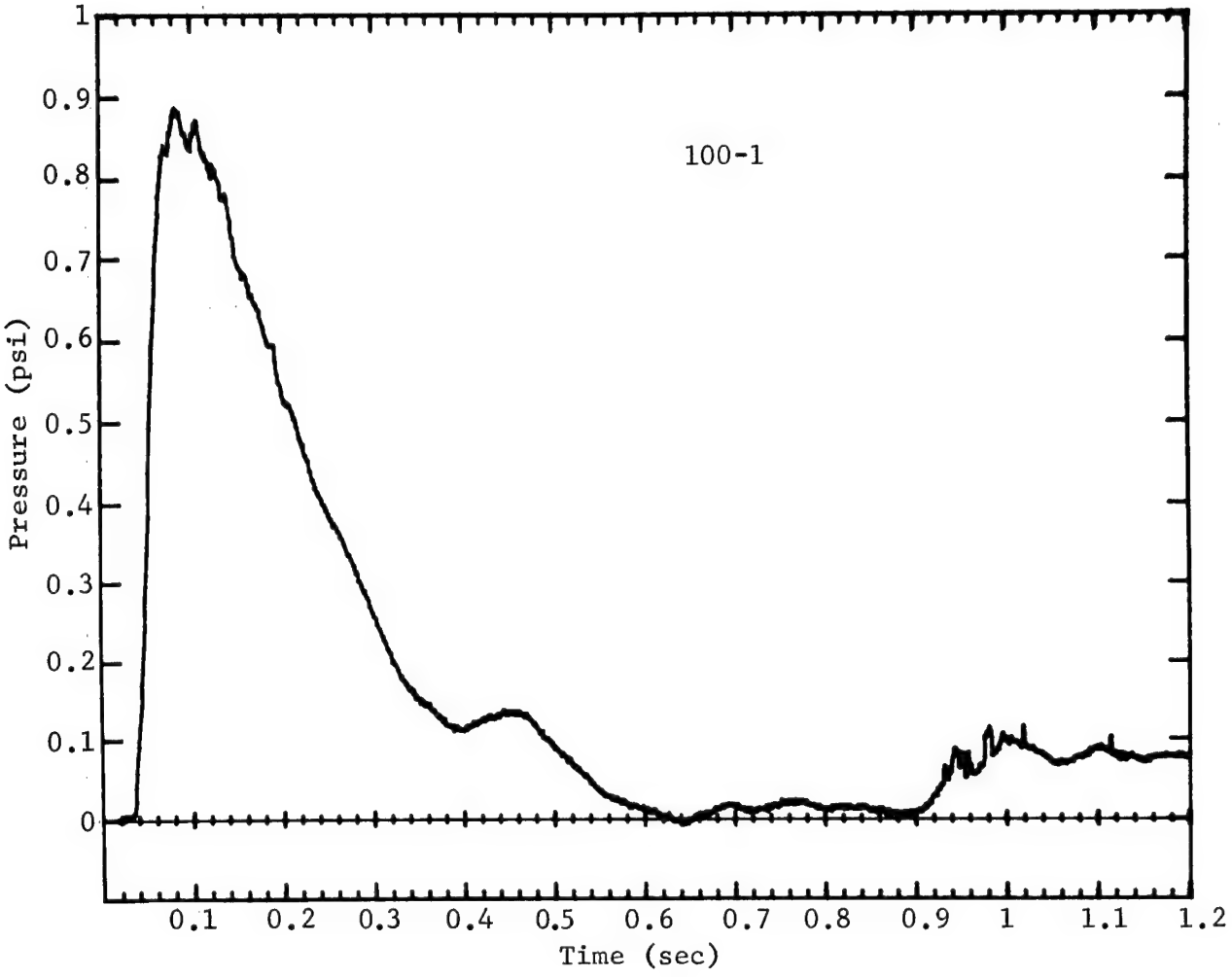

Figure A.4

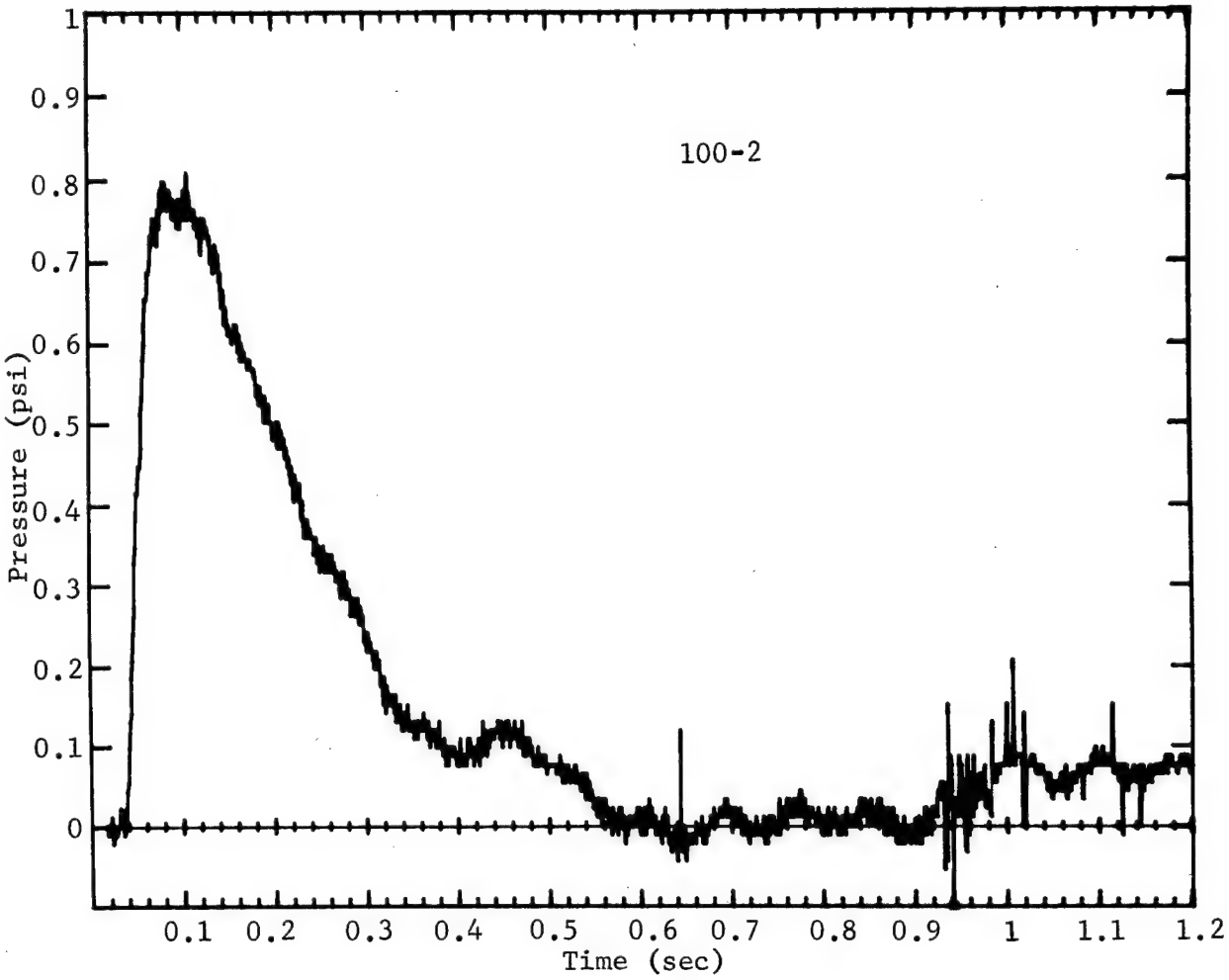
100-2
Pressure (psi)
Time (sec)
1
0.9
0.8
0.7
0.6
0.5
0.4
0.3
0.2
0.1
0
0.1 0.2 0.3 0.4 0.5 0.6 0.7 0.8 0.9 1 1.1 1.2

Figure A.5

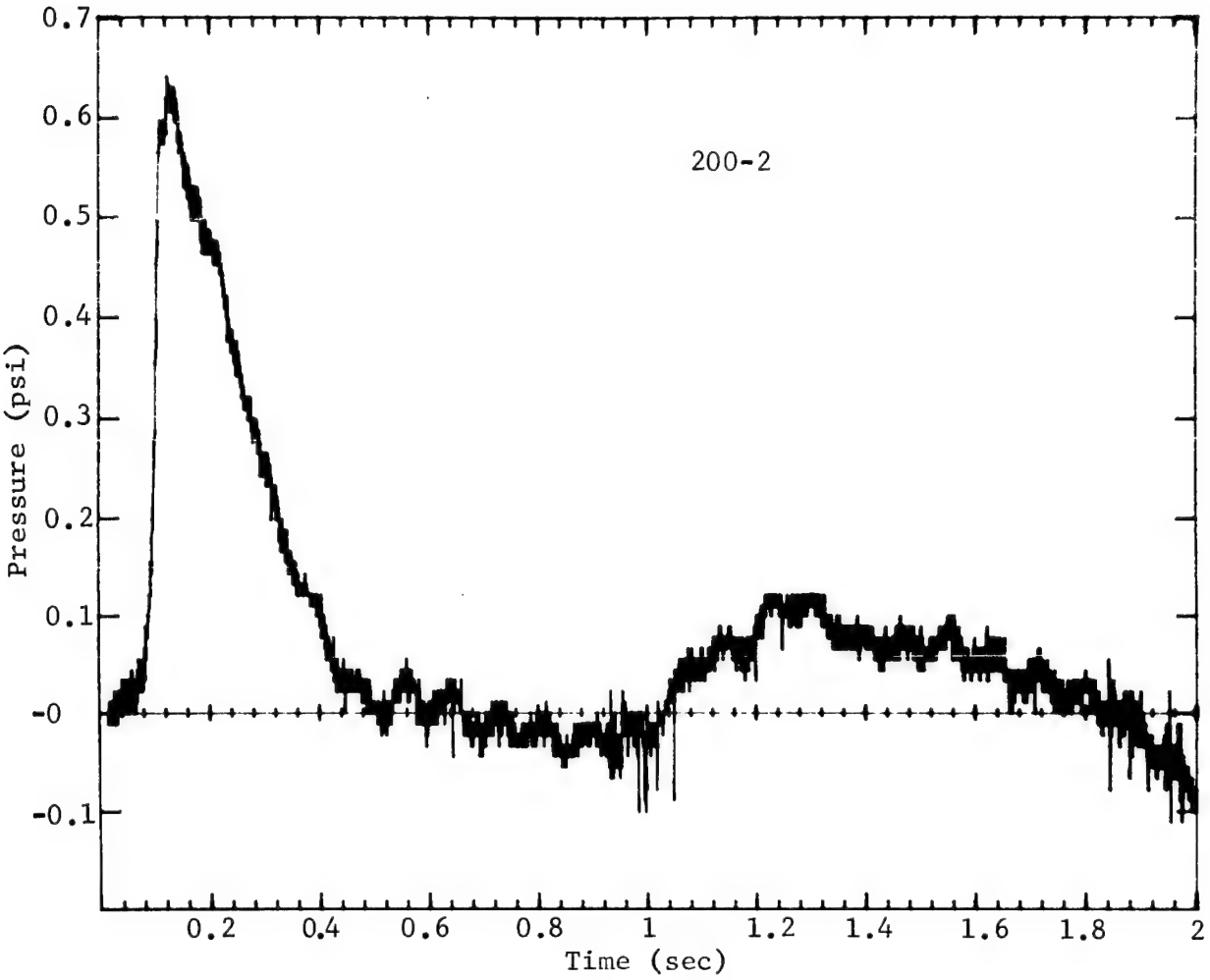
200-2
Pressure (psi)
0.7
0.6
0.5
0.4
0.3
0.2
0.1
-0
-0.1
0.2
0.4
0.6
0.8
1
1.2
1.4
1.6
1.8
2
Time (sec)

Figure A.6

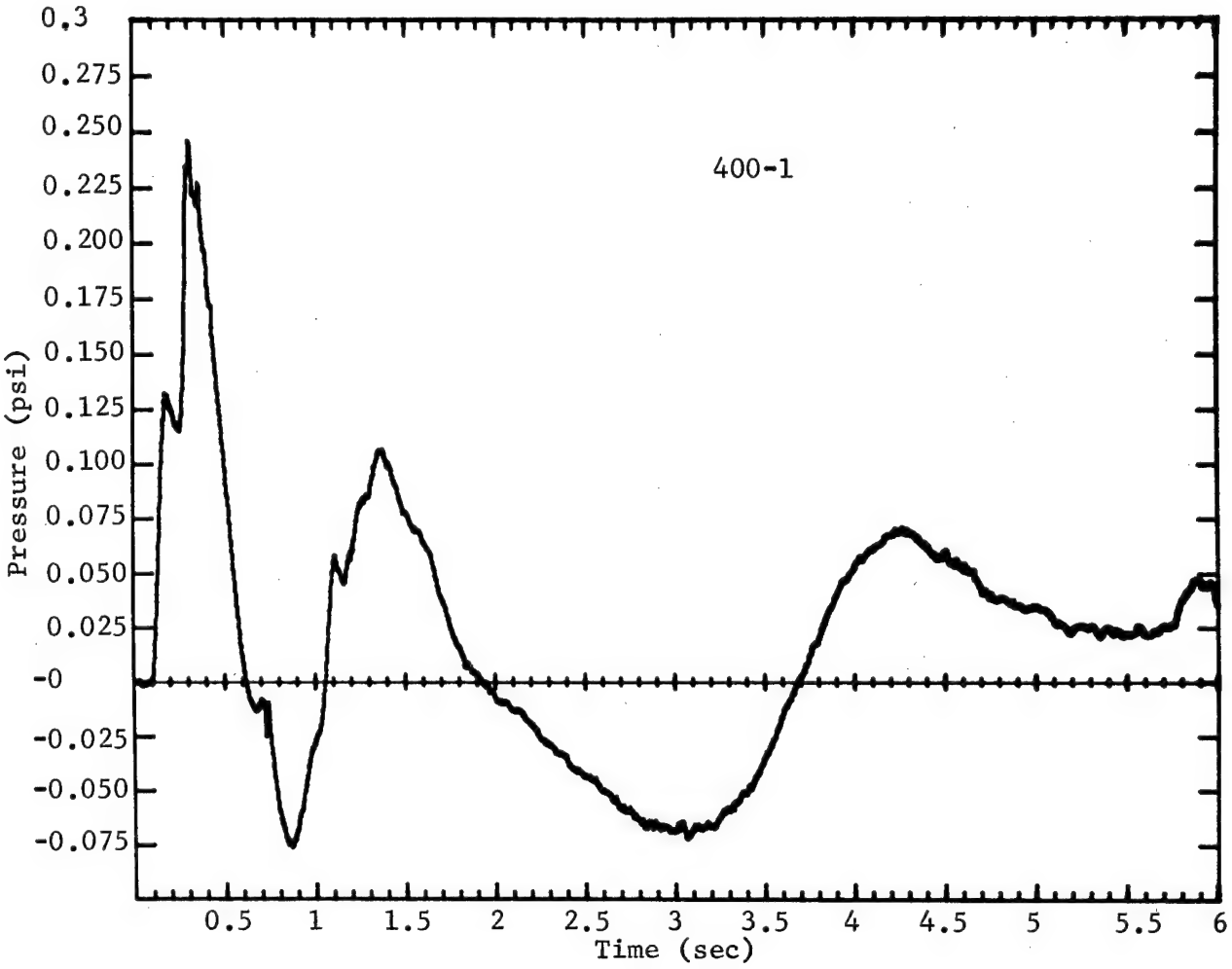
400-1
Pressure (psi)
0.3
0.275
0.250
0.225
0.200
0.175
0.150
0.125
0.100
0.075
0.050
0.025
-0
-0.025
-0.050
-0.075
0.5
1
1.5
2
2.5
3
3.5
4
4.5
5
5.5
6
Time (sec)

Figure A.7

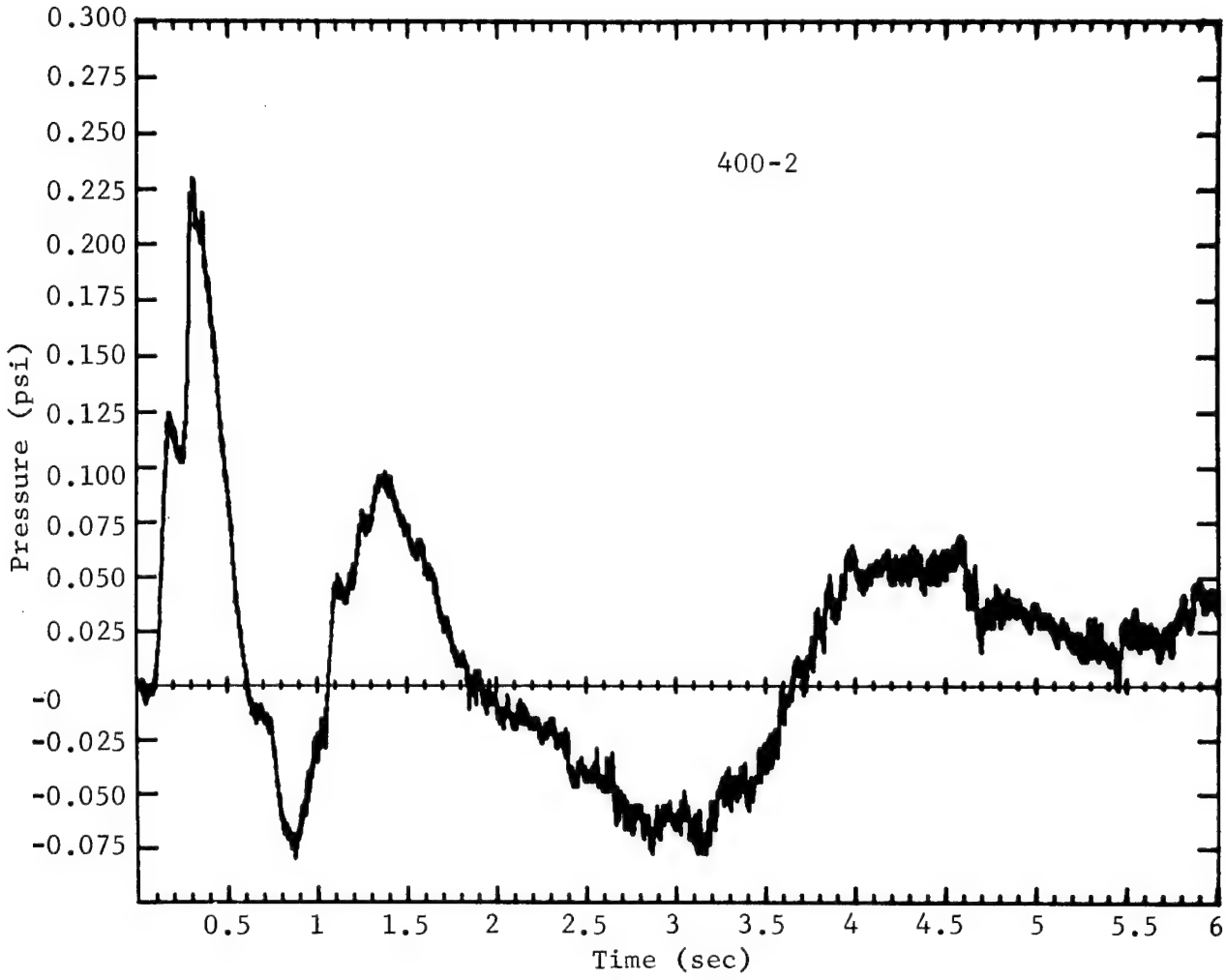
400-2
Pressure (psi)
0.300
0.275
0.250
0.225
0.200
0.175
0.150
0.125
0.100
0.075
0.050
0.025
-0
-0.025
-0.050
-0.075
0.5
1
1.5
2
2.5
3
3.5
4
4.5
5
5.5
6
Time (sec)

Figure A.8

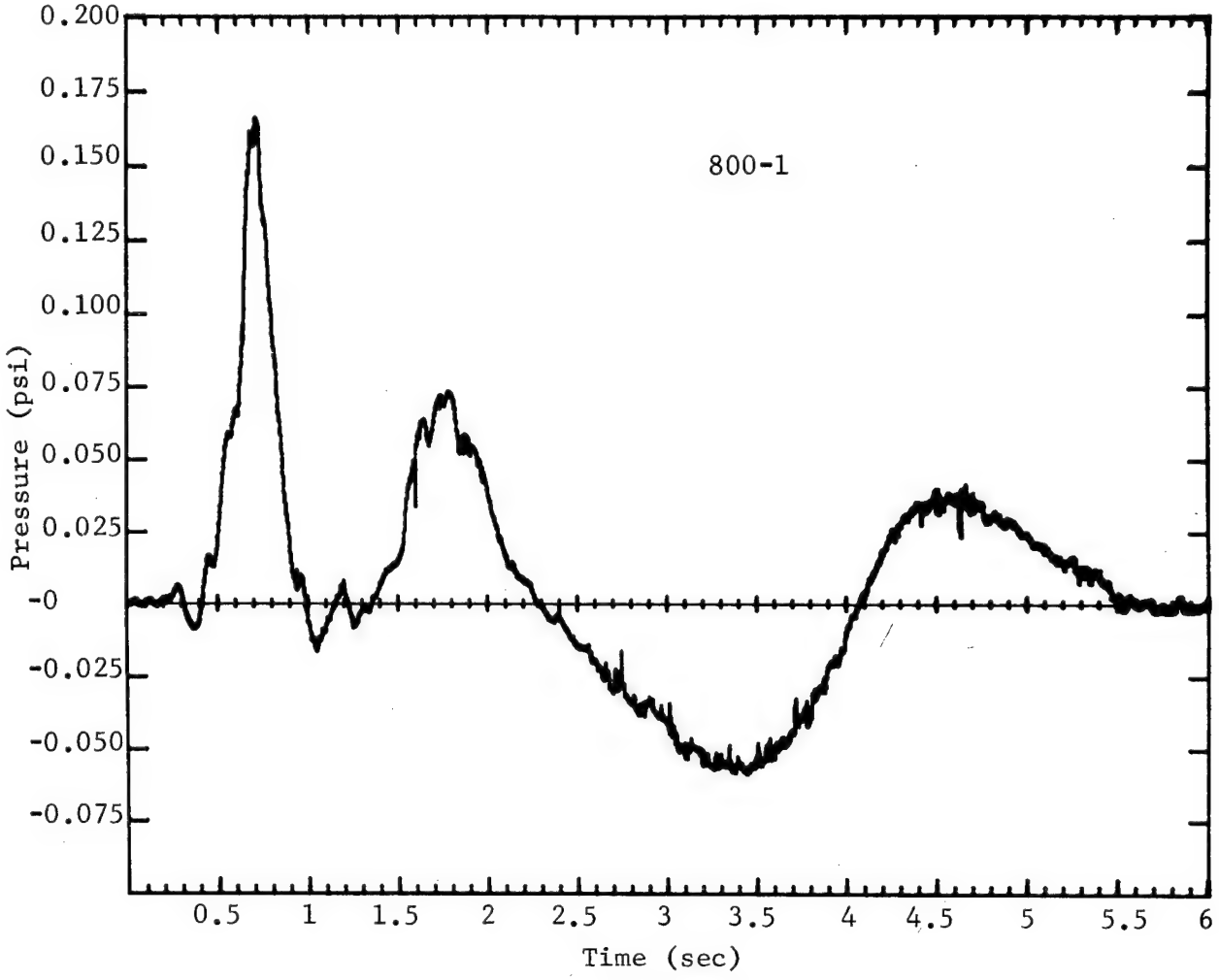
800-1
0.200
0.175
0.150
0.125
0.100
0.075
0.050
0.025
-0
-0.025
-0.050
-0.075
Pressure (psi)
0.5
1
1.5
2
2.5
3
3.5
4
4.5
5
5.5
6
Time (sec)

Figure A.9

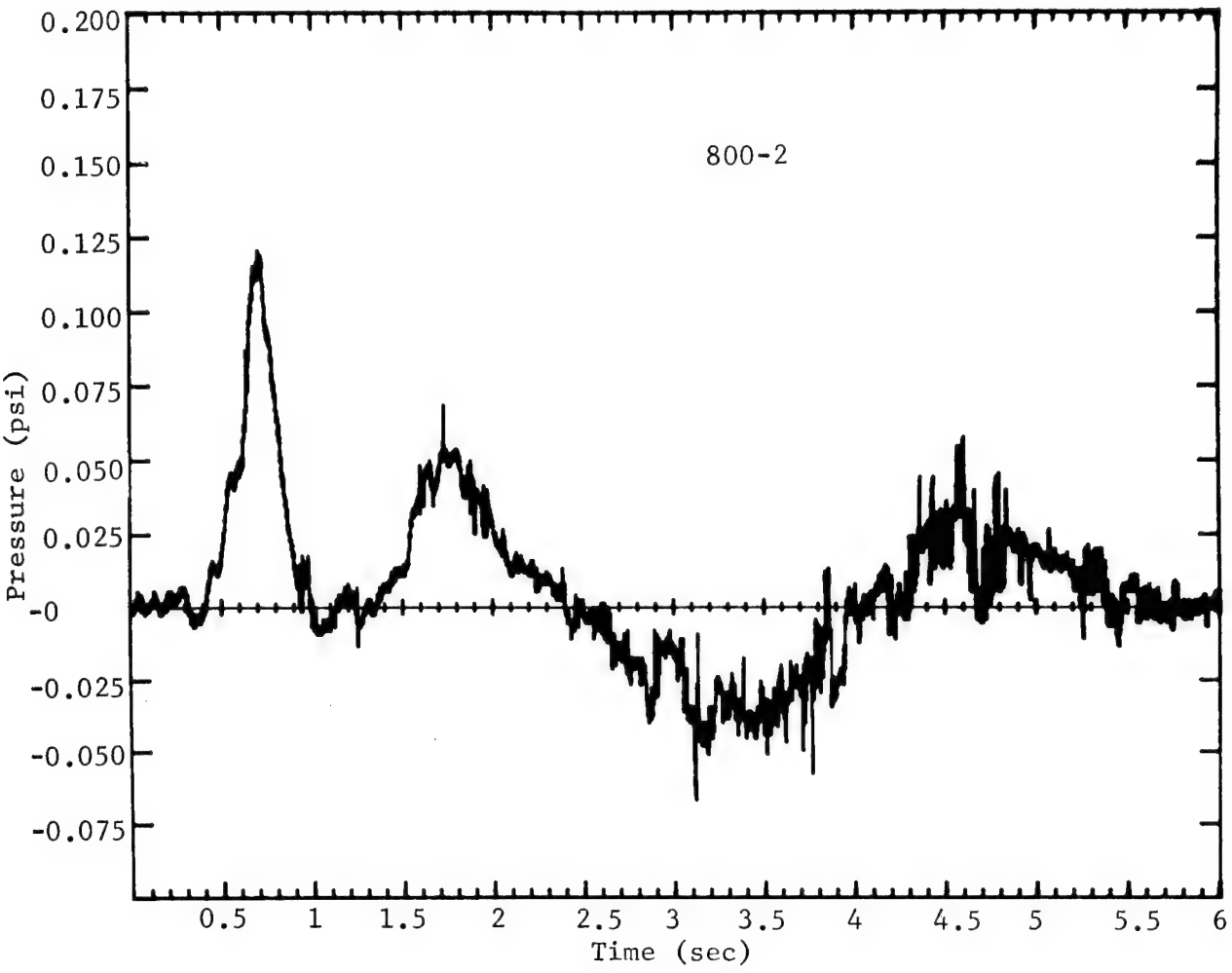
800-2
Pressure (psi)
0.200
0.175
0.150
0.125
0.100
0.075
0.050
0.025
-0
-0.025
-0.050
-0.075
0.5
1
1.5
2
2.5
3
3.5
4
4.5
5
5.5
6
Time (sec)

Figure A.10

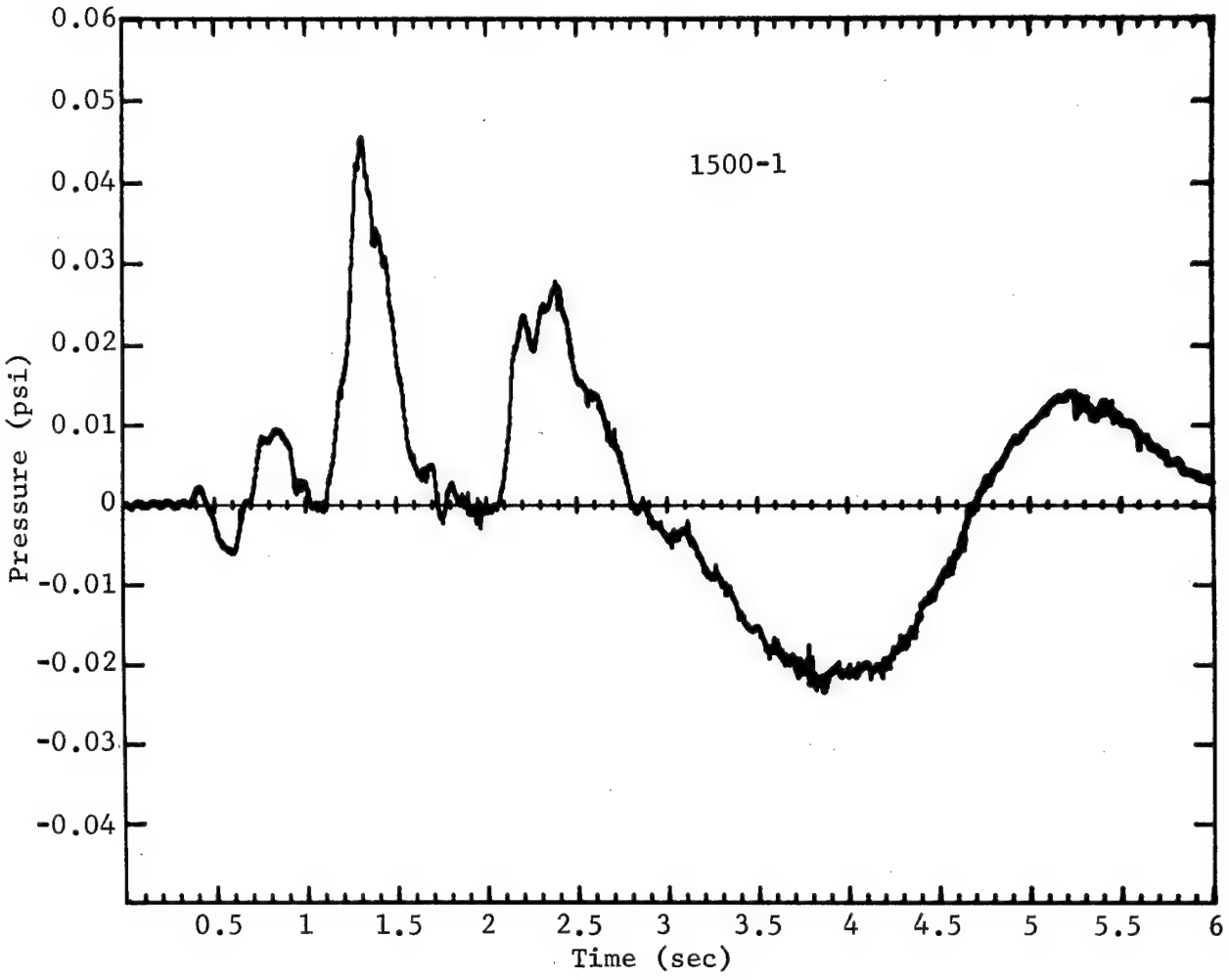
1500-1
Pressure (psi)
0.06
0.05
0.04
0.03
0.02
0.01
0
-0.01
-0.02
-0.03
-0.04
0.5
1
1.5
2
2.5
3
3.5
4
4.5
5
5.5
6
Time (sec)

Figure A.11

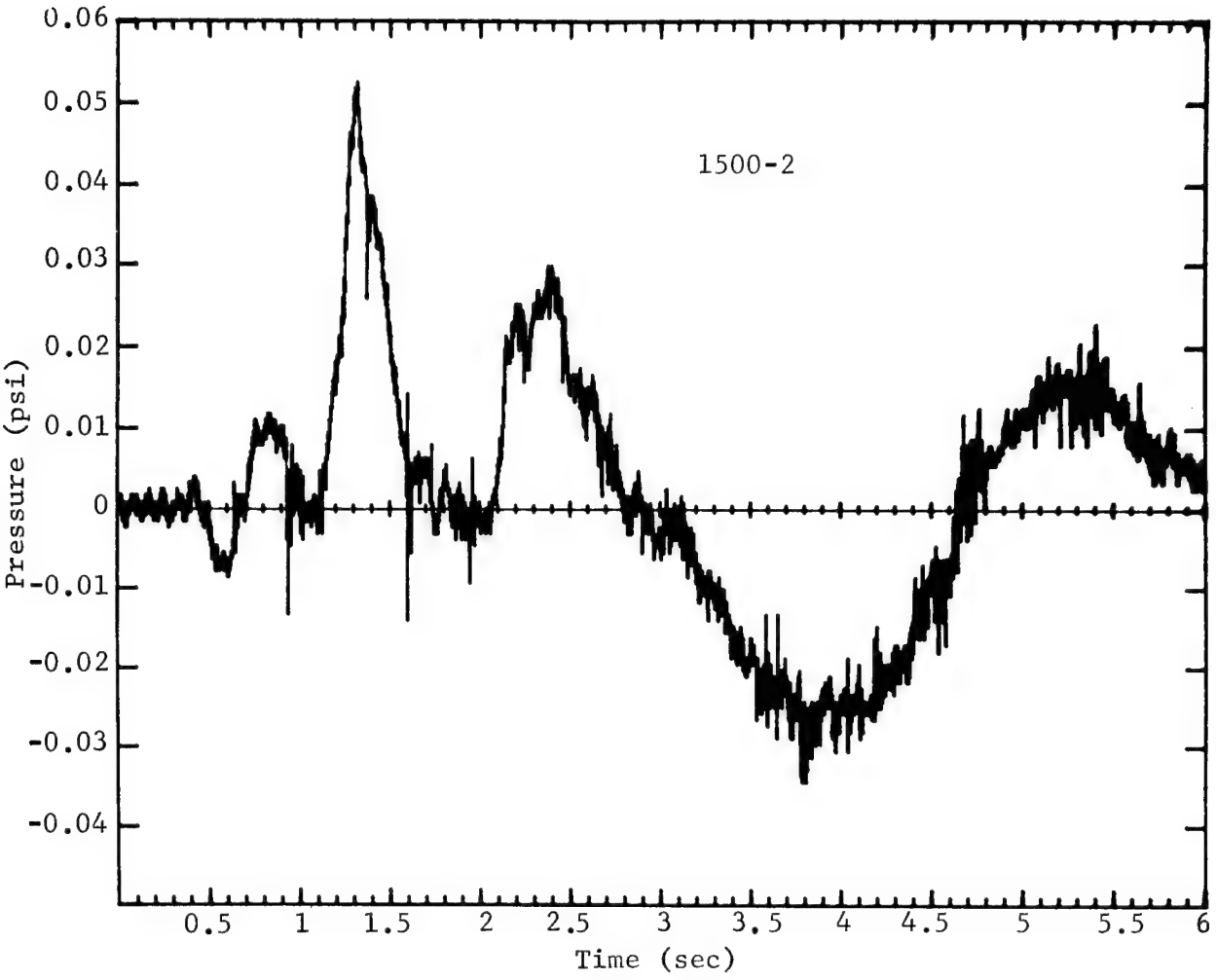
1500-2
Pressure (psi)
0.06
0.05
0.04
0.03
0.02
0.01
0
-0.01
-0.02
-0.03
-0.04
0.5
1
1.5
2
2.5
3
3.5
4
4.5
5
5.5
6
Time (sec)

Figure A.12

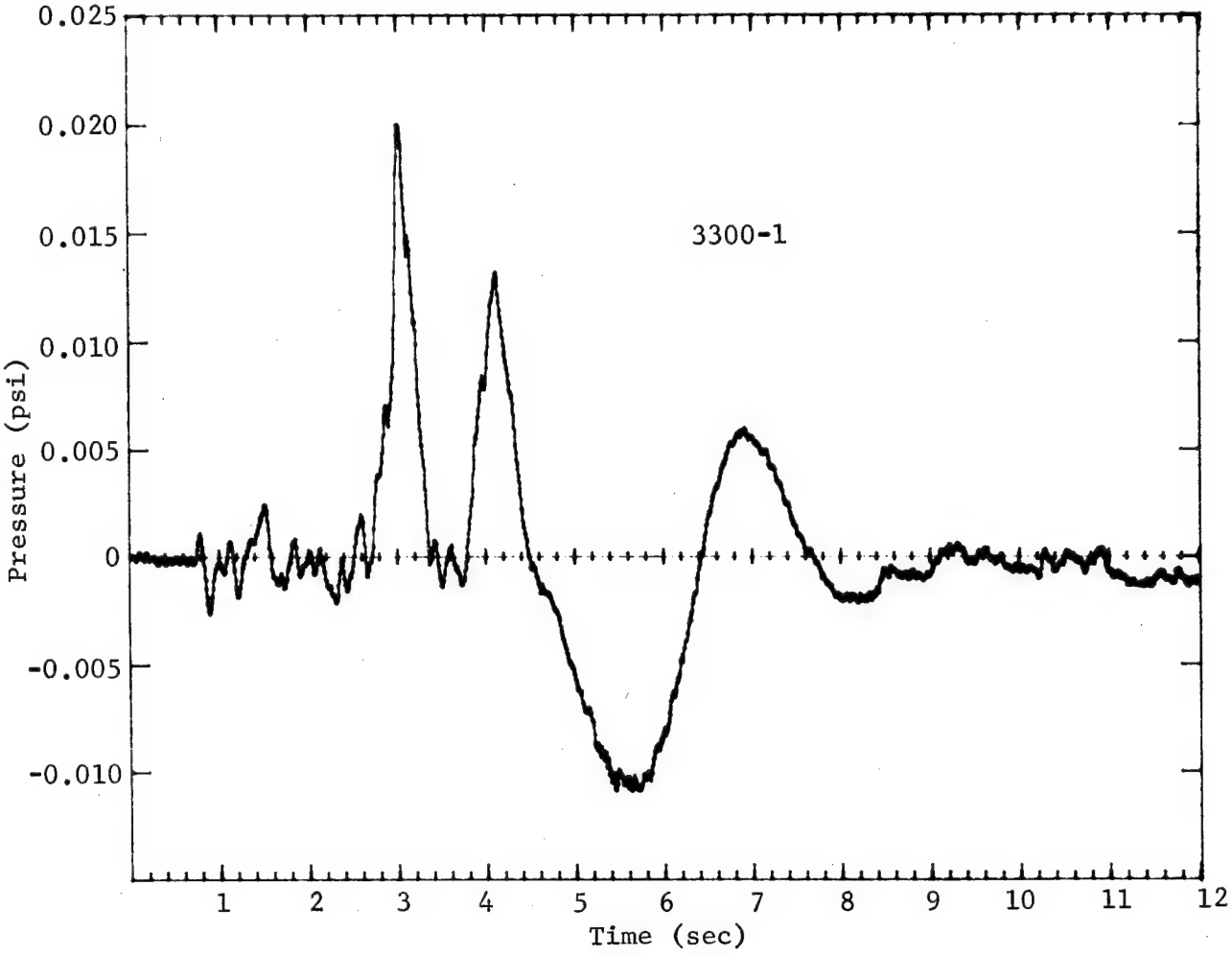
0.025
0.020
0.015
0.010
0.005
0
-0.005
-0.010
Pressure (psi)
3300-1
1
2
3
4
5
6
7
8
9
10
11
12
Time (sec)

Figure A.13

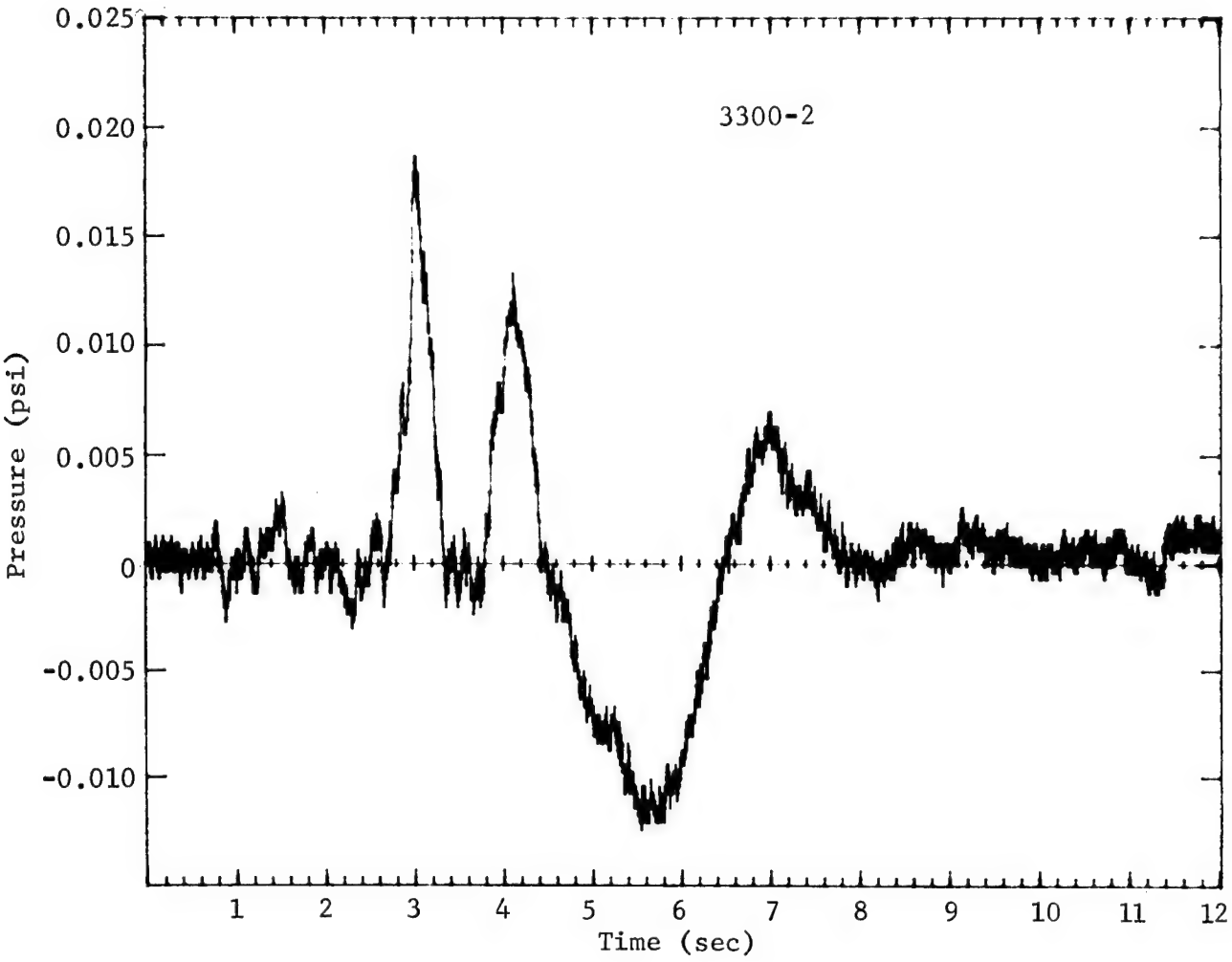
3300-2
0.025
0.020
0.015
0.010
0.005
0
-0.005
-0.010
Pressure (psi)
1
2
3
4
5
6
7
8
9
10
11
12
Time (sec)

Figure A.14

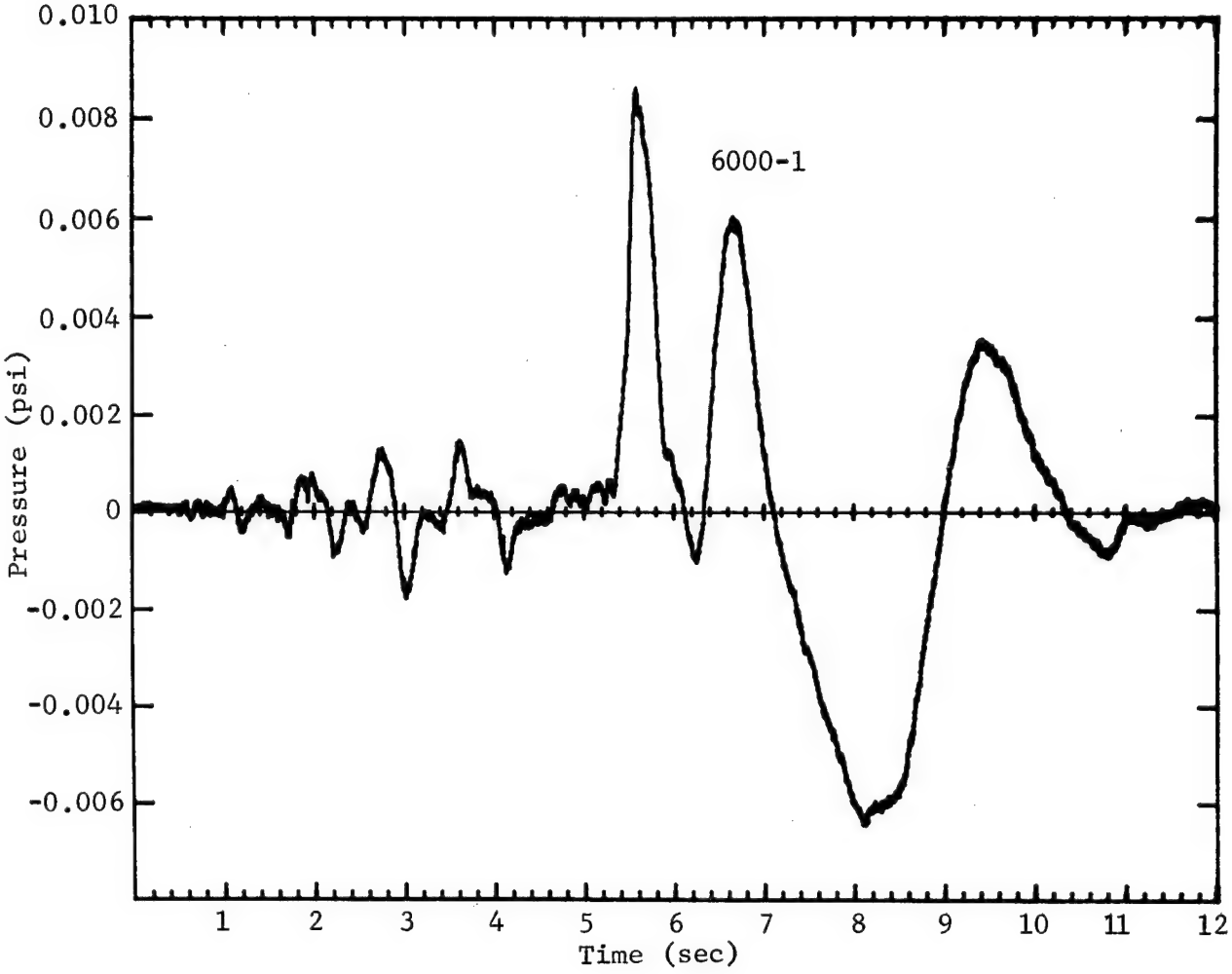
0.010
0.008
0.006
0.004
0.002
0
-0.002
-0.004
-0.006
Pressure (psi)
6000-1
1
2
3
4
5
6
7
8
9
10
11
12
Time (sec)

Figure A.15

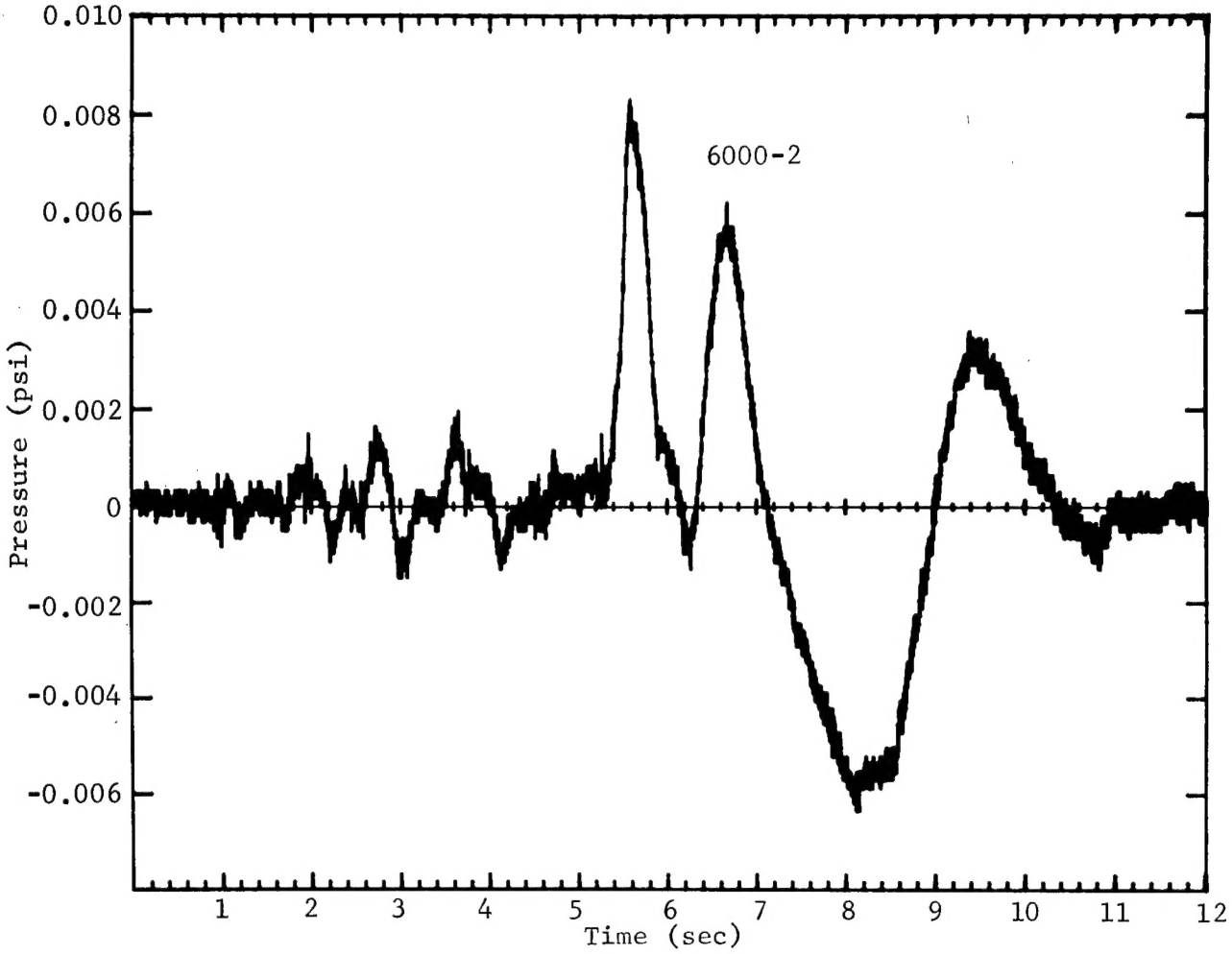
0.010
0.008
0.006
0.004
0.002
0
-0.002
-0.004
-0.006
Pressure (psi)
6000-2
1
2
3
4
5
6
7
8
9
10
11
12
Time (sec)

Figure A.16

PROJECT CABRIOLET REPORTS

Report	Agency	Author	Title
PNE-950	LRL		Cabriolet Summary
PNE-951	Sandia, Albu	L. Vortman	Close-In Air Blast
PNE-952	Sandia, Albu	J. Reed	Long-Range Air Blast
PNE-953	LRL	L. Ramspott	Cabriolet Pre-Shot Geology
PNE-954	WES	R. W. Hunt D. M. Bailey L. D. Carter	Preshot Geological Engineering Investigation for Project Cabriolet, Pahute Mesa, NTS

TENTATIVE REPORTS

LRL	T. Gibson	Ground Radiation Survey
LRL	R. Rohrer	Cloud and Surface Measurements
LRL	R. Marks	Subsurface Effects
NCG		Crater Topography

DISTRIBUTION LIST
(TID-4500, Category UC-35)

No. Copies	
1	AEC ALBUQUERQUE OPERATIONS OFFICE
1	AEC BETHESDA TECHNICAL LIBRARY
25	AEC DIVISION OF PEACEFUL NUCLEAR EXPLOSIVES
1	AEC LIBRARY, WASHINGTON
1	AEC MISSION TO THE IAEA
5	AEC NEVADA OPERATIONS OFFICE
1	AEC NEW YORK OPERATIONS OFFICE
1	AEC PATENT OFFICE
5	AEC SAN FRANCISCO OPERATIONS OFFICE
1	AEC SAVANNAH RIVER OPERATIONS OFFICE
1	AEC SCIENTIFIC REPRESENTATIVE, BELGIUM
1	AEC SCIENTIFIC REPRESENTATIVE, ENGLAND
1	AEC SCIENTIFIC REPRESENTATIVE, JAPAN
1	AEROSPACE CORPORATION, SAN BERNARDINO (AF)
1	AIR FORCE AERO PROPULSION LABORATORY (APE)
1	AIR FORCE FOREIGN TECHNOLOGY DIVISION
1	AIR FORCE INSTITUTE OF TECHNOLOGY
1	AIR FORCE SCHOOL OF AEROSPACE MEDICINE
1	AIR FORCE WEAPONS LABORATORY
1	AMES LABORATORY (AEC)
1	ARGONNE NATIONAL LABORATORY (AEC)
8	ARMY ABERDEEN PROVING GROUND
1	ARMY CHIEF OF ENGINEERS
1	ARMY ELECTRONICS COMMAND
1	ARMY ENGINEER DIVISION
5	ARMY ENGINEER NUCLEAR CRATERING GROUP
6	ARMY ENGINEER WATERWAYS EXPERIMENT STATION
1	ARMY MATERIEL COMMAND
1	ARMY MEDICAL FIELD SERVICE SCHOOL
1	ARMY MEDICAL RESEARCH UNIT
1	ARMY MOBILITY EQUIPMENT RESEARCH AND DEVELOPMENT CENTER
1	ARMY NUCLEAR DEFENSE LABORATORY
1	ARMY PICATINNY ARSENAL
1	ARMY ROCKY MOUNTAIN ARSENAL
1	ARMY SURGEON GENERAL
1	ARMY WALTER REED MEDICAL CENTER
1	ATOMIC POWER DEVELOPMENT ASSOCIATES, INC. (AEC)
2	ATOMICS INTERNATIONAL (AEC)
1	BABCOCK AND WILCOX COMPANY, WASHINGTON (AEC)
2	BATTELLE MEMORIAL INSTITUTE (AEC)
1	BATTELLE-NORTHWEST (AEC)
1	BROOKHAVEN NATIONAL LABORATORY (AEC)
2	BUREAU OF MINES, BARTLESVILLE (INT)
1	BUREAU OF MINES, DENVER (INT)
1	BUREAU OF MINES, LARAMIE (INT)
6	BUREAU OF RECLAMATION (INT)
1	DEPARTMENT OF AGRICULTURE NATIONAL LIBRARY
1	DOD DASA LIVERMORE
1	DOD DASA RADIOBIOLOGY RESEARCH INSTITUTE
1	DOD DASA SANDIA
1	DOD DASA WASHINGTON
1	DU PONT COMPANY, AIKEN (AEC)
1	DU PONT COMPANY, WILMINGTON (AEC)
1	EG&G, INC., ALBUQUERQUE (AEC)
1	EG&G, INC., LAS VEGAS (AEC)
5	EL PASO NATURAL GAS COMPANY
8	ENVIRONMENTAL RESEARCH CORPORATION (AEC)
1	ENVIRONMENTAL RESEARCH CORPORATION, LAS VEGAS (AEC)
1	ENVIRONMENTAL SCIENCE SERVICES ADMINISTRATION, LAS VEGAS (COMM.)
1	ENVIRONMENTAL SCIENCE SERVICE ADMINISTRATION, MARYLAND (COMM.)

No. Copies	
1	FRANKFORD ARSENAL (P-D LABS.)
1	GENERAL DYNAMICS/FORT WORTH (AF)
1	GENERAL ELECTRIC COMPANY, CINCINNATI (AEC)
1	GENERAL ELECTRIC COMPANY, SAN JOSE (AEC)
1	GEOLOGICAL SURVEY, DENVER
1	GEOLOGICAL SURVEY, FLAGSTAFF (INT)
1	GEOLOGICAL SURVEY, MENLO PARK (INT)
1	GEOLOGICAL SURVEY (PECORA) (INT)
1	GULF GENERAL ATOMIC INCORPORATED (AEC)
2	HOLMES AND NARVER, INC. (AEC)
1	HUGHES AIRCRAFT COMPANY, FULLERTON (ARMY)
1	INSTITUTE FOR DEFENSE ANALYSIS (ARMY)
1	ISOTOPES, INC. (AEC)
1	JET PROPULSION LABORATORY (NASA)
1	LAWRENCE RADIATION LABORATORY, BERKELEY (AEC)
4	LAWRENCE RADIATION LABORATORY, LIVERMORE (AEC)
2	LOS ALAMOS SCIENTIFIC LABORATORY (AEC)
5	LOVELACE FOUNDATION (AEC)
1	MATHEMATICA (AEC)
1	MUESER, RUTLEDGE, WENTWORTH AND JOHNSTON (AEC)
1	MUTUAL ATOMIC ENERGY LIABILITY UNDERWRITERS (AEC)
1	NASA JOHN F. KENNEDY SPACE CENTER
1	NATIONAL BUREAU OF STANDARDS (LIBRARY)
1	NATIONAL INSTITUTES OF HEALTH (HEW)
1	NATIONAL REACTOR TESTING STATION (INC) (AEC)
1	NAVY ATOMIC ENERGY DIVISION
1	NAVY OFFICE OF NAVAL RESEARCH (CODE 422)
2	NAVY ORDNANCE LABORATORY
1	NAVY ORDNANCE SYSTEMS COMMAND
1	NAVY POSTGRADUATE SCHOOL
1	NAVY RADIOLOGICAL DEFENSE LABORATORY
1	NAVY SHIP SYSTEMS COMMAND HEADQUARTERS
1	NRA, INC.
4	OAK RIDGE NATIONAL LABORATORY (AEC)
1	OCEANOGRAPHIC SERVICES, INC. (AEC)
1	OHIO STATE UNIVERSITY (OCD)
3	PUBLIC HEALTH SERVICE, LAS VEGAS (HEW)
1	PUBLIC HEALTH SERVICE, MONTGOMERY (HEW)
1	PUBLIC HEALTH SERVICE, ROCKVILLE (HEW)
1	PUBLIC HEALTH SERVICE, WINCHESTER (HEW)
1	PUERTO RICO NUCLEAR CENTER (AEC)
1	PURDUE UNIVERSITY (AEC)
1	RADIOPTICS, INC. (AEC)
2	REYNOLDS ELECTRICAL AND ENGINEERING COMPANY, INC. (AEC)
4	SANDIA CORPORATION, ALBUQUERQUE (AEC)
1	SANDIA CORPORATION, LIVERMORE (AEC)
1	SOUTHWEST RESEARCH INSTITUTE (AEC)
1	STANFORD UNIVERSITY (AEC)
1	TENNESSEE VALLEY AUTHORITY
1	UNION CARBIDE CORPORATION (ORGDP) (AEC)
1	UNIVERSITY OF CALIFORNIA, DAVIS, TALLEY (AEC)
1	UNIVERSITY OF MICHIGAN (VESIAC) (ARMY)
1	UNIVERSITY OF ROCHESTER (KAPLON) (AEC)
1	UNIVERSITY OF TENNESSEE (AEC)
1	UNIVERSITY OF WASHINGTON (AEC)
1	WASHINGTON STATE UNIVERSITY (AEC)
1	WESTINGHOUSE ELECTRIC CORPORATION, MC KENNA (AEC)
66	AEC DIVISION OF TECHNICAL INFORMATION EXTENSION
25	CLEARINGHOUSE FOR FEDERAL SCIENTIFIC AND TECHNICAL INFORMATION

PROJECT CABRIOLET

DISTRIBUTION LIST

1 D. J. Convey, Department of Mines and Technical Surveys, Ottawa, Ontario, Canada
1 Dr. G. W. Govier, Oil and Gas Conservation Board, Calgary, Alberta, Canada
1 U. S. Army Engineer Division, Lower Mississippi Valley, P. O. Box 80, Vicksburg, Mississippi 39181
1 U. S. Army Engineer District, 668 Federal Office Building, Memphis, Tennessee 38103
1 U. S. Army Engineer District, P. O. Box 60267, New Orleans, Louisiana 70160
1 U. S. Army Engineer District, 906 Olive Street, St. Louis, Missouri 63101
1 U. S. Army Engineer District, P. O. Box 60, Vicksburg, Mississippi 39181
1 U. S. Army Engineer Division, APO N. Y. 09019, Leghorn, Italy
1 U. S. Army Engineer District, GULF, APO N. Y. 09205, Teheran, Iran
1 U. S. Army Engineer Division, P. O. Box 103, Downtown Station, Omaha, Nebraska 68101
1 U. S. Army Engineer District, 1800 Federal Office Building, Kansas City, Missouri 64106
1 U. S. Army Engineer District, 6012 U. S. Post Office & Court House, 215 No. 17th Street, Omaha, Nebraska 68101
1 U. S. Army Engineer Division, 424 Trapelo Road, Waltham, Massachusetts 02154
1 U. S. Army Engineer Division, 90 Church Street, New York, New York 10007
1 U. S. Army Engineer District, P. O. Box 1715, Baltimore, Maryland 21203
1 U. S. Army Engineer District, 111 East 16th Street, New York, New York 10003
1 U. S. Army Engineer District, Ft. Norfolk, 803 Front Street, Norfolk, Virginia 23510
1 U. S. Army Engineer District, Custom House, 1nd & Chestnut Street, Philadelphia, Pennsylvania 19106
1 U. S. Army Engineer Division, 536 S. Clark Street, Chicago, Illinois 60605
1 U. S. Army Engineer District, Foot of Bridge Street, Buffalo, New York 14207
1 U. S. Army Engineer District, 219 S. Dearborn Street, Chicago, Illinois 60604
1 U. S. Army Engineer District, P. O. Box 1027, Detroit, Michigan 48231
1 U. S. Army Engineer District, Clock Tower Building, Rock Island, Illinois 61202
1 U. S. Army Engineer District, 1217 US PO & Customhouse, St. Paul, Minnesota 55101
1 U. S. Army Engineer District, Lake Survey, 630 Federal Building, Detroit, Michigan 48226
1 U. S. Army Engineer Division, 210 Custom House, Portland, Oregon 97209
1 U. S. Army Engineer District, 628 Pittock Block, Portland, Oregon 97205
1 U. S. Army Engineer District, P. O. Box 7002, Anchorage, Alaska 99051
1 U. S. Army Engineer District, 1519 Alaska Way, South, Seattle, Washington 98134
1 U. S. Army Engineer District, Building 602, City-County Airport, Walla Walla, Washington 99362
1 U. S. Army Engineer Division, P. O. Box 1159, Cincinnati, Ohio 45201
1 U. S. Army Engineer District, P. O. Box 2127, Huntington, West Virginia 25721
1 U. S. Army Engineer District, P. O. Box 59, Louisville, Kentucky 40201
1 U. S. Army Engineer District, P. O. Box 1070, Nashville, Tennessee 37202
1 U. S. Army Engineer District, 2032 Federal Building, 1000 Liberty Avenue, Pittsburg, Pennsylvania 15222
1 U. S. Army Engineer Division, Building 96, Fort Armstrong, Honolulu, Hawaii 96813
1 U. S. Army Engineer District, Far East, APO, San Francisco, California 96301
1 U. S. Army Engineer District, Building 96, Fort Armstrong, Honolulu, Hawaii 96813
1 U. S. Army Engineer District, Okinawa, APO, San Francisco, California 96331
1 U. S. Army Engineer Division, 510 Title Building, 30 Pryor Street SW., Atlanta, Georgia 30303
1 U. S. Army Engineer District, P. O. Box 1042, Merritt Island, Florida 32952
1 U. S. Army Engineer District, P. O. Box 905, Charleston, South Carolina 29402
1 U. S. Army Engineer District, P. O. Box 4970, Jacksonville, Florida 32201
1 U. S. Army Engineer District, P. O. Box 1169, Mobile, Alabama 36601
1 U. S. Army Engineer District, P. O. Box 889, Savannah, Georgia 31402
1 U. S. Army Engineer District, P. O. Box 1890, Wilmington, North Carolina 28402
1 U. S. Army Engineer Division, 630 Sansome Street, Room 1216, San Francisco, California 94111
1 U. S. Army Engineer District, P. O. Box 17277, Foy Station, Los Angeles, California 90017
1 U. S. Army Engineer District, 650 Capitol Mall, Sacramento, California 95814
1 U. S. Army Engineer District, 100 McAllister Street, San Francisco, California 94102
1 U. S. Army Engineer Division, 1114 Commerce Street, Dallas, Texas 75202
1 U. S. Army Engineer District, P. O. Box 1538, Albuquerque, New Mexico 87103
1 U. S. Army Engineer District, P. O. Box 1600, Fort Worth, Texas 76101
1 U. S. Army Engineer District, P. O. Box 1229, Galveston, Texas 77551
1 U. S. Army Engineer District, P. O. Box 867, Little Rock, Arkansas 72203
1 U. S. Army Engineer District, P. O. Box 61, Tulsa, Oklahoma 74102
1 U. S. Army Liaison Detachment, 111 E. 16th Street, New York, New York 10003
1 Mississippi River Commission, P. O. Box 80, Vicksburg, Mississippi 39181
1 Rivers and Harbors, Boards of Engineers, Temp C Building, 2nd & Q Streets SW., Washington, D. C. 20315
1 Corps of Engineer Ballistic Missile Construction Office, P. O. Box 4187, Norton Air Force Base, California 92409
1 U. S. Army Engineer Center, Ft. Belvoir, Virginia 22060
1 U. S. Army Engineer School, Ft. Belvoir, Virginia 22060
1 U. S. Army Engineering Reactors Group, Ft. Belvoir, Virginia 22060
1 U. S. Army Engineer Training Center, Ft. Leonard Wood, Missouri 65473
1 U. S. Coastal Engineering Research Board, 5201 Little Falls Road NW., Washington, D. C. 20016
75 U. S. Army Engineer Waterways Experiment Station, Vicksburg, Mississippi 39180
50 U. S. Army Engineer Nuclear Cratering Group, Livermore, California 94551